EFFECT OF PROCESSING VARIABLES ON PHYSICO – CHEMICAL PROPERTIES OF BASMATI RICE – PIGEONPEA EXTRUDATES

By

RAJAY JAYANTILAL TERAIYA

A thesis submitted to the

Graduate School-New Brunswick

Rutgers, The State University of New Jersey

in partial fulfillment of the requirements

for the degree of

Master of Science

Graduate Program in Food Science

written under the direction of

Dr. Mukund V. Karwe

and approved by

_____

_____

_____

New Brunswick, New Jersey

October, 2012

ABSTRACT OF THE THESIS

Effect of processing variables on physico – chemical properties of

Basmati rice – pigeonpea extrudates

By Rajay Teraiya

Thesis Director:

Dr. Mukund V. Karwe

Extrusion of pigeonpea and Basmati rice was carried out to find out if there are optimum extrusion conditions in terms of the processing variables that give desirable physico – chemical properties to extrudates. Pigeonpea is a nutritionally dense legume. Because extrusion can produce low moisture and long shelf life products, it would be useful to make pigeonpea available to wider market. High protein content of pigeonpea may limit its use as an extrudable material because high proteins concentration usually curtails expansion. Basmati rice, being a traditional supplement and rich in starch, can provide an aid for expansion when mixed with pigeon pea flour.

A Brabender single screw extruder was employed for the extrusion of Basmati rice and pigeonpea flour mixture. Four factors of importance chosen for this study were: ratio of whole pigeonpea to Basmati rice (25 % to 75 %), barrel temperature (120 °C-160 °C), moisture content (19- 24 %), and screw speed (120-180 RPM). Response surface methodology (central composite design, CCD) was first used to design experiments. Based on results of the CCD design, a three factor Box-Behnken design (BBD) was employed which focused on the impact of three major parameters, namely, the temperature of the barrel (120 °C-160 °C), the moisture content (19- 24 %) and the screw speed (120-180 RPM) on extrudate properties.

The fraction of pigeonpea in the mixture that could provide acceptable exapanded product with sufficient amount of protein was 0.5 or 50%. The processability was not significantly affected up to 50 % pigeonpea in the mixture. The particle size distribution (PSD) had significant effect on the physico-chemical properties of extrudate.

Moisture content of the finished product was inversely proportional to the barrel temperature. An increase in temperature and/or screw speed caused a decrease in bulk density of the extrudate. Water solubility index (WSI) and water absorption index (WAI) increased with increase in barrel temperature. WSI was also influenced by fraction of pigeonpea in the mixture with a positive correlation. An increase in the screw speed reduced the brown color and increased the brightness of the extrudate to some extent.

ACKNOWLEDGEMENT

I am extremely thankful to Dr. Karwe for granting me the opportunity to work in this project. Throughout this project he gave me his valuable advice, moral and financial support, without which I would not have completed my research.

I am thankful to Dr. Kit Yam and Dr. Michael Rogers for serving on my thesis committee. I am also thankful to all of my teachers and professors for helping me broaden my knowledge and understanding.

Operation of the extruder would not be possible without constant support of Mr. Dave Petrenka and Mr. Frank Caira. I have learnt many valuable engineering skills from them which helped me to get through my research and will continue to help me in future.

I am grateful to Leco Corporation, Michigan, USA for performing proximate analysis and amino acid analysis of Basmati rice and pigeonpea.

I am thankful to all of my lab mates for their constant support and encouragement throughout my research. Without them and my other friends I would not be able to achieve the goals that I have achieved.

I would also like to extend my gratitude to my parents, my brother and his family for their love and support.

And I also give thanks to my one and only true love, Lisa, who stuck by me and inspired me to move forward with my research.

Finally, I thank God for making me the person who I am and for giving me the strength to go through thick and thin of life.

TABLE OF CONTENTS

LIST OF FIGURES

LIST OF TABLES

1. INTRODUCTION

1.1 Introduction to pigeonpea:

Pigeonpea (*Cajanus cajan*) is known by many names such as: in English: “cango pea”, “angola pea”, “goongo”, “puertorico pea” and “red gram” (Morton, 1976); in Urdu and Hindi: “arhar”; in Marathi: “Tur”; in Guajarati: “Tuver”; in Tamil: “Thuvai” and in Telugu: “Kandus”. Pigeonpea gains its name due to its appeal to wild pigeons (Hulse, 1991). It is a sustainable, draught tolerant legume grown in tropical and sub-tropical regions of the world. One of the oldest grown crops, it ranks fifth in importance among legumes (Morton, 1976 and Whiteman, 1985). Pigeonpea constitutes 6.5 % of the world’s total pulses area and contributes 5.7 % to the total pulses production. The crop has its origin in India and spread to Africa more than 4000 years ago (Van der maesen, 1980).

India consumes 85 % of world pigeonpea supply. Consumption of pigeonpea in India is mainly done after dehusking and cooking in the form of dhal (decorticated split cotyledons). Other countries where pigeonpea is an important legume are Kenya, Uganda, Malawi, Thailand and Philippines. In contrast to the way it is consumed in India, African countries generally consume whole pigeonpea after boiling. Pigeonpea contains 17.9 to 24.3 % protein (wet basis or w.b.), depending upon the cultivar. Majority of its protein (~65 % w.b.) is in the form of globulin and is not rich in sulfur containing amino acids (Singh, 1982). Although the albumin fraction represents a small portion of pigeonpea protein, it is also rich in sulfur containing amino acids such as Cystine and Methionine, which are essential amino acids for humans and are the limiting amino acids for legumes (Singh, 1984). Lack of these amino acids can be compensated by proper

selection of cultivars that are high in glutelin as compared to globulin (Singh, 1982). The second important consideration is anti-nutritional factors or anti-physiological substances that have a potential to be the source of low protein digestibility. Trypsin inhibitors, chymotrypsin inhibitors, amylase inhibitors and polyphenols are very important for pigeonpea. Trypsin inhibitors in pigeonpea are lower in content as compared to soy bean and lima bean. Some of the protease inhibitors in pigeonpea are heat labile and can be denatured by cooking. Cooking under acidic condition is shown to denature the protein inhibitors in pigeonpea (Liener, 1979 and Singh, 1984). Condensed tannins in the range of 0.0 to 0.2 % (w.b.) (Price, 1980) are present along with other polyphenols in pigeonpea. These polyphenols are shown to inhibit trypsin, chymotrypsin and amylase enzymes (Singh, 1984). Inhibitory effect of pigeonpea cultivar with dark seed coat color was found to be significantly higher as compared to the cultivars with light seed coat color. It has been shown that seed coat colors influence the protein quality of beans, heat resistant tannins and other polyphenols, which act as trypsin inhibitors (Elias, 1979). Therefore, pigeonpea cultivar with light seed coat color was chosen for the current study.

It is shown that during the process of milling (i.e., de-hulling the pigeonpea) to prepare “dahl” reduces the protein content and quality (Singh, 1980). This is attributed to the removal of the outer layers that are rich in protein (Reddy, 1979). They are lost due to abrasive action of the roller mill during processing. Therefore, whole pigeonpea was used for the current study. Whole pigeonpea is brownish in appearance and approximately spherical in shape with average size of half centimeter in diameter. Pigeonpea used for extrusion are shown in Figure 1.1. Internal structure of pigeonpea is comparable to pea as shown in Figure 1.2 (Finch-Savage, 2006).

Figure 1.1 Whole pigeonpea seeds (dried)

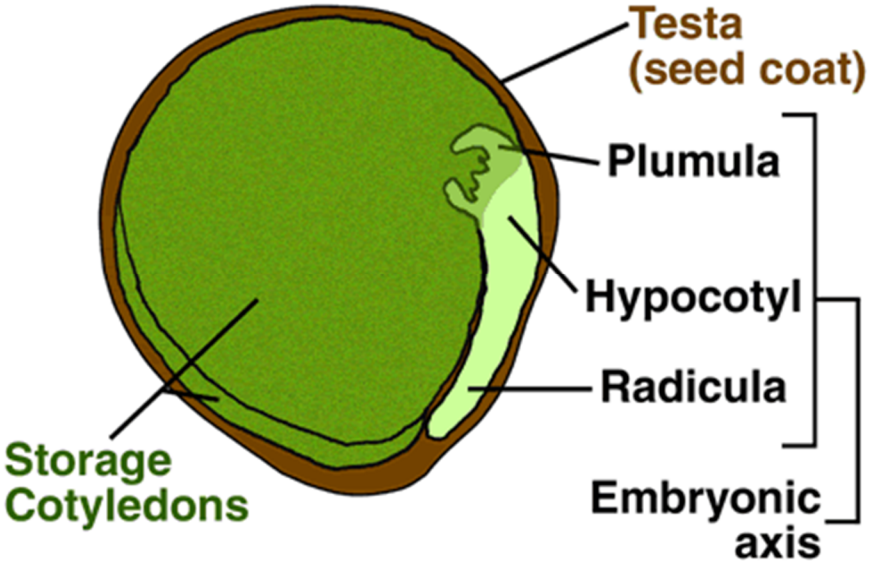

Figure 1.2 Whole pea (*Pisum sativum*) cross section

Proximate composition of pigeonpea is given in Table 1.1.

Table 1.1 Nutritional composition of pigeonpea (fresh and dried)

Nutrient	Percentage (w. b.) (Fresh)	Percentage (w. b.) (Dried)
Protein	7.20	19.20
Lipid	1.64	4.37
Ash	1.40	3.37
Water	65.88	9.00
Carbohydrates by difference	23.88	63.69

Source: Data for fresh pigeonpea is from USDA nutrient database. Data for dried pigeonpea is calculated by assuming the moisture content to be 9 % (w.b.). (Site: http://www.nal.usda.gov/fnic/foodcomp/cgi-bin/list_nut_edit.pl, download date June 24, 2011)

Pigeonpea being a legume also fixates the nitrogen from atmosphere to earth. This reduces/eliminates the need for nitrogen-rich chemical fertilizer (e.g., ammonium nitrate).

Traditional preparation (i.e., dahl) being high in moisture content of around 59 % (as per USDA database, http://www.nal.usda.gov/fnic/foodcomp/cgi-bin/list_nut_edit.pl, download date June 24, 2011) has a very limited shelf life. An extrusion process could convert it into a dried snack enhancing its exposure to wider population. The high protein content of pigeonpea limits its extrudability. Since legumes are difficult to extrude alone, they are combined with cereals with a high starch content to make them more extrudable (Iwe, 1998; Rampersad, 2003).

1.2 Introduction to Basmati rice

Rice, a traditional supplement to pigeonpea, was selected as an extrusion aid. It is rich in starch content (approximately 80 %). The use of rice in extruded products is increasing due to its nutrition, hypoallergenicity, colorlessness and bland taste (Chrastil, 1992). Rice protein has a unique hypoallergenic (hypo - less than normal) properties and ranks high in nutritive quality (rich in the essential amino acid lysine) among the cereal proteins (Bean, 1985). Amongst many varieties of rice, Basmati rice was selected for extrusion due to its aromatic properties. Additionally, Basmati rice has better protein quality and amino acid content when compared to non-scented varieties (Sekhar and Reddy, 1982). Basmati rice is a long grain variety of rice. Proximate composition of Basmati rice is given in Table 1.2

Table 1.2 Proximate composition of Basmati rice

Nutrient	% (w. b.)
Protein	7.13
Lipid	0.66
Ash	0.64
Water	11.62
Carbohydrates by difference	79.95

Source: USDA nutrient database.

(Site: http://www.nal.usda.gov/fnic/foodcomp/cgi-bin/list_nut_edit.pl, download date June 24, 2011)

Figure 1.3 Basmati rice grain

Basmati rice grain has an elongated shape and depending on degree of polishing after hull removal, is brownish to white in color. Basmati rice used for extrusion is shown in Figure 1.3.

A major portion of rice (between 80 to 90 %) is starch. It is in the form of a compound polyhedral granule ranging from 3 to 9 µm (Juliano, 1985). Starch in general consists of branched (amylopectin) and linear (amylose) fractions. The majority of starch in rice is amylopectin. Depending on amount of linear fraction of milled rice, it is categorized as waxy: 1-2 %; low: 7-20 %; intermediate: 20-25 % and high :> 25 % (Juliano, 1979). Amylose content is inversely proportional to the final viscosity of gelatinized starch (Juliano, 1982). Starch undergoes gelatinization and forms a viscous liquid that can flow through the extruder and entrap the expanded moisture upon exiting

the extruder. This is makes starch (and in turn rice) an expansion aid. Rice starch granules are microcrystalline and show the characteristic Maltese cross under polarized light (Zobel, 1964).

In terms of chemical constituents, excluding water, protein is the next major fraction in rice. Three (of the four) major fraction of rice protein are albumin, globulin and glutelin with iso-electric pHs of 4.1, 4.3 and 7.9, respectively. Prolamin being the fourth fraction of rice protein is not precipitable by pH adjustment however it can be precipitated using acetone. Of the total protein content of rice, albumin, globulin, glutelin and prolamin are 4.45, 13.11, 79.74 and 2.46 % (Ju, 2001).

Detailed internal structure and organization of rice was investigated by Blakeney (1984) and is shown in Figure 1.4.

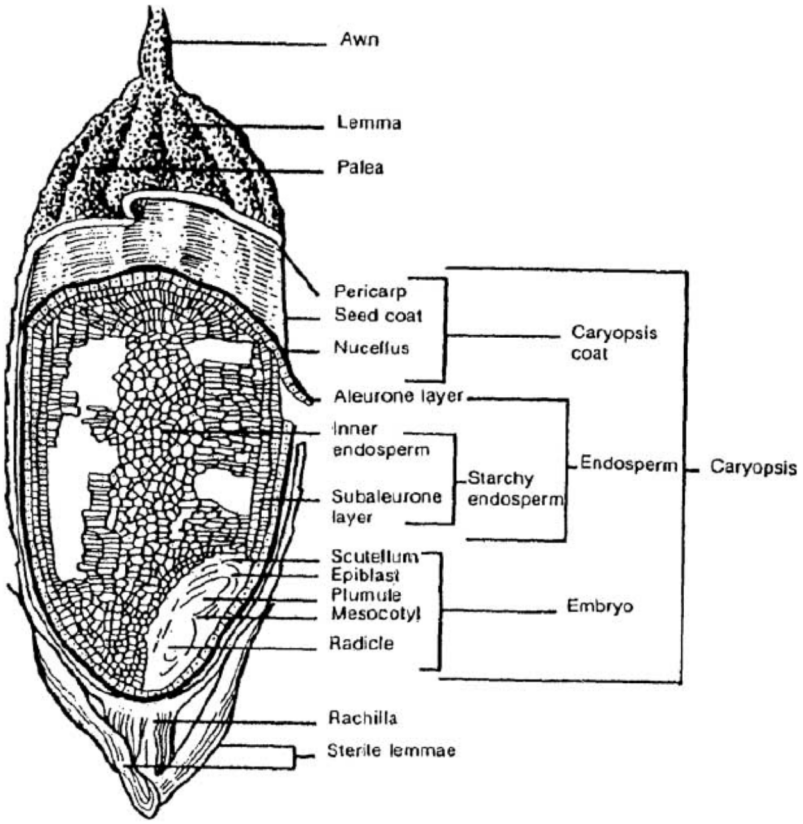

Figure 1.4 Detailed structure of rice (Blakeney, 1984)

1.3 Introduction to extrusion

To extrude means to shape (a material) by forcing it through a die. Extruders are utilized to manufacture many food products such as, baby foods, beverage bases, biscuits, bread dough, breakfast cereals, chocolate, confectionaries, modified starches, pasta, pet foods, snacks and textured proteins.

Basic principles of extrusion were used in Harappan civilization in 2500 B.C. to extrude steatite glass beads (Hedge and others, 1982). Rolling and sheeting process would date back to antiquity (Harper, 1981). Pushing a flow through a perforated device dates back to 9th century A.D. with the southern Indian process of forcing viscous dough of wheat in sweetened milk through a hole made in the base of a coconut shell. (Achaya, 1998).

Barrel-ram arrangements were recorded as early as 1154 A.D. in Sicily, by an Arab traveler named Idrisi for pasta manufacturing (Agnesi, 1996). During the industrial revolution extruded pasta quickly became a staple food in southern Italy (McGee, 1984).

In the food industry single screw and twin screw extruder are used predominantly. In either case, the screw(s) are contained in a barrel, which provides heating and cooling and an orifice at the end, called the “die”. The barrel is divided in separate zones to maintain the required temperature profile. The feed material passes through distinct phases while travelling through an extruder. Based on the material state and function, these zones are termed: solid transport zone, melt zone and pump zone.

In a typical extrusion process, a batch or a continuous pre-conditioner is used for moisture adjustments. The raw material enters a hopper that feeds the material to the

extruder barrel. Rotating screw(s) push the material down the barrel and out of the die. Figure 1.5 illustrates a typical single screw extruder. Although the figure represents a constant bore diameter and increasing core/root diameter they both can be varied to achieve desired extrudate characteristics. The ratio of volume developed by axial area in one revolution at the feed to the same at the end is termed as compression ratio. In food extrusion industry screws having 1:1 to 1:3 compression ratio are used. Decreasing pitch, threaded barrel, conical barrel and alternating pin type screw are other geometries being used in extrusion industry (Riaz, 2000).

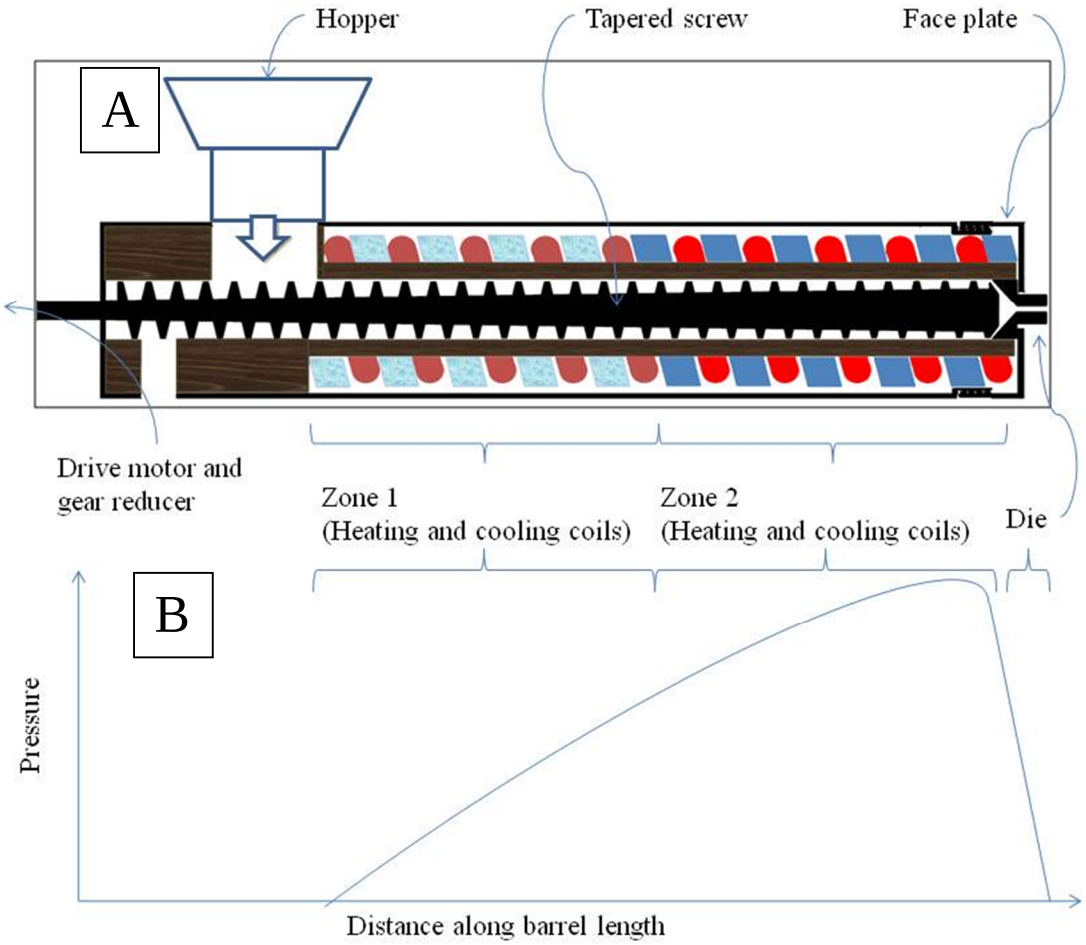

Figure 1.5 Mechanical features of a two zone, single screw extruder showing a tapered screw and simplified diagram of pressure buildup during extrusion

Due to increasing core diameter the material passing through extruder gets compacted. This results in an increased pressure as illustrated in Figure 1.5 B. In addition to the pressure increase heat is generated by viscous dissipation (heat generated due to the friction at the boundary wall and by internal friction) as well as conductive heat transfer from barrel resulting in higher temperature. The starch portion of the feed is gelatinized, proteins are denatured, some of the anti-nutrition factors and enzymes are inhibited, free lipids get bound to starch and vitamins and antioxidants are denatured.

Unlike conventional batch processes such as, cookers, ovens and stirred tank reactors, extrusion is a high-temperature short-time (HTST) process. In addition to conduction or convection, during extrusion heat is generated due to shear forces exerted by the screw on the material being conveyed. Extruders can sometimes be classified as a scraped surface heat exchanger (Mercier, 1989).

In addition to extruder design, chemical composition of extruder feed has an influence on the extrudate characteristics. The composition of the feed is comprised of starch, protein and lipid as the major components of its matrix. Fraction and quality of each component in the extruder feed affects finished product properties.

1.4 Effect of Starch on extrusion

Starch plays an important role in extrudability and texture of extruded food products. During extrusion high temperature and mechanical shear cause starch to undergo gelatinization. To understand gelatinization we need to understand starch chemistry.

Starch is formed by glycosidic linkages between a large number of glucose molecules. Based on the type of the linkage it is either linear (amylose with α (1→4) linkage, roughly 20-25 % of total starch content) or branched (amylopectin with branches forming at α (1→6) linkage, roughly 4 -5 % of the glucose units of amylopectin form this linkage). Roughly 10^6 glucose molecules form amylopectin while 10^3 glucose units form a helix of amylose. The reducing end with linear and branch linkages forms the nucleus of the starch granule, which is called the C chain. From the C chain, branched and linear linkages form the majority of structure (amorphous in nature), which is called as the B chain. Periphery of the starch granule comprises of the straight linkages termed as the A chain (Campbell-platt, 2009). This structure is best understood by the cluster model as shown in Figure 1.6.

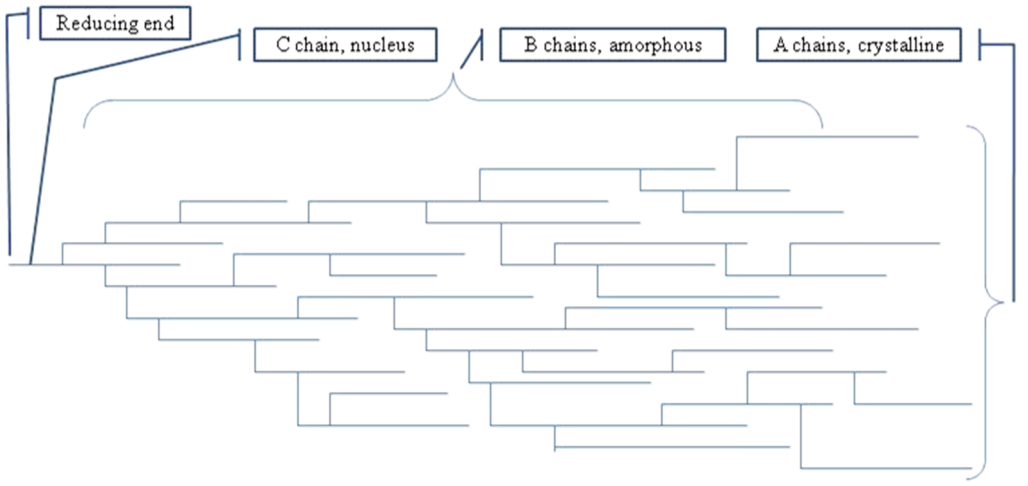

Figure 1.6 Amylopectin cluster model (adapted from: Campbell-platt, 2009)

When starch granules are subjected to elevated temperature at high moisture condition, the granules begin to absorb water and expand and thus lose their structure. As expanded starch granules occupy more space and make the free water bind to its

monosaccharide units and increases the viscosity of the suspension. Amylose that is embedded into the starch granule (not shown in the Figure 1.6) is released, increasing the viscosity further in the process. Upon cooling amylose and amylopectin form a gel like structure via the formation of hydrogen bonds. Gelatinization changes the structure of rice starch granule drastically, which can be best seen in SEM (scanning electron microscope) images at different temperature, as shown in Figure 1.7.

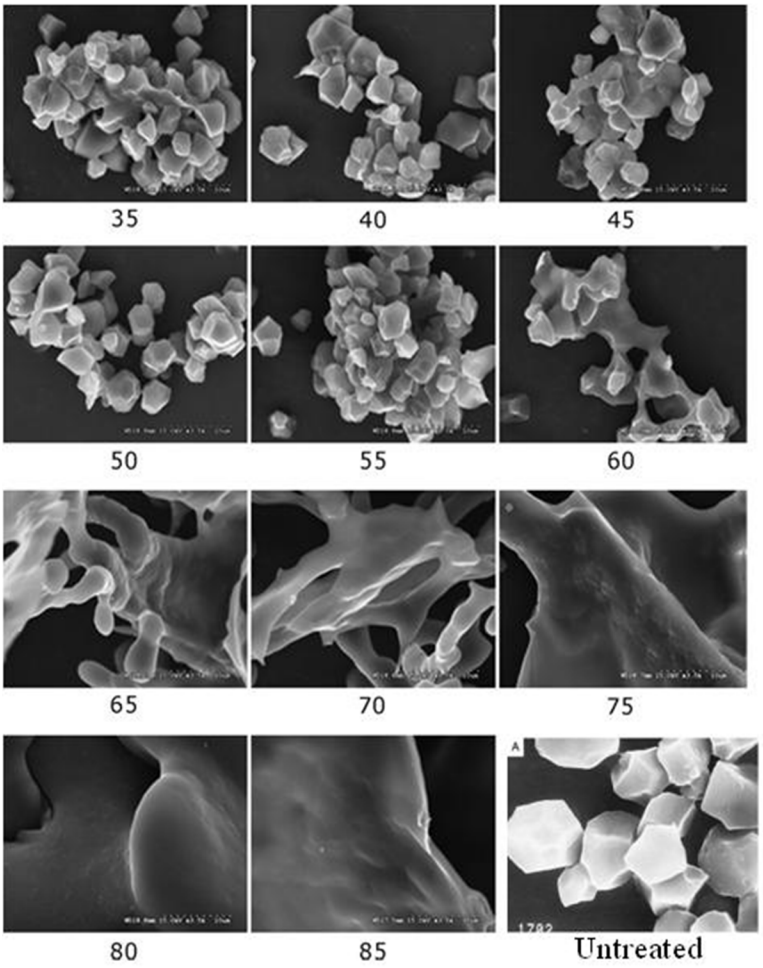

Figure 1.7 Scanning electron microscopic images of untreated rice starch granule (18 % w.b. moisture) labeled as 'Untreated" at 1000 X magnification (Singh, 2005) and treated rice starch (the number below each Figure represents the treatment temperature (ºC)) at 2500 X magnification (Ratnayake, 2006).

Gelatinization, melting and denaturation cause change in the physical properties of starch due to formation of a new molecular aggregate structure by hydrogen bonding. This causes initial rapid rise in the viscosity, which in turn increases the pressure of melt at the die. Once the extruder reaches the peak the viscosity, a steady decline in viscosity (and thus pressure) is noted as the melt is further heated and mechanically sheared till stabilization of the material flow through the extruder. Depending on the severity of process condition fragmentation and formation of complexes may follow (Akdogan, 1997). Rice starch gelatinization temperature range is 68 to 78 ºC (Hodge and Osman, 1976). Gelatinization temperature range is defined as the range of temperature when starch granules start to swell in hot water, accompanied by a loss of birefringence (Juliano, 1982; Hizukuri, 1983). Since the extrusion is usually conducted above 100 ºC, in addition to gelatinization of starch, degradation, fragmentation and melting are expected. Shear forces physically disrupt the starch granules causing penetration of water into the granules. Destruction of starch granule increases with increase in temperature and shearing action (Barron, 2001).

As shown in the Figure 1.8, typical starchy flour goes from the glassy region to the rubbery region upon moisture addition. Heating during extrusion brings it into free flow region. Flash-off at the end of extrusion and further drying brings the product back in to the glassy region and provides the crunchy texture (Karwe, 2003).

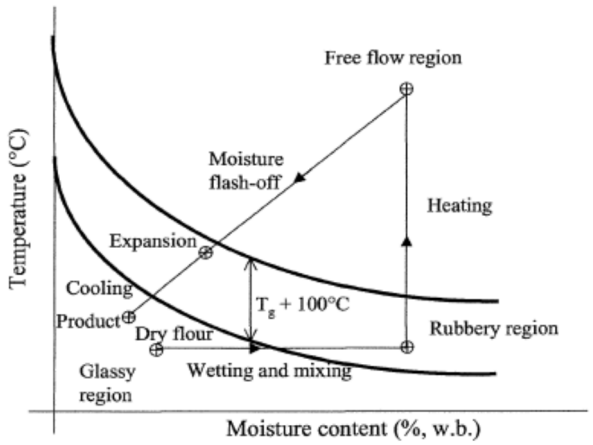

Figure 1.8 Phase diagram for cereal starches and proteins, and path of extrusion process (Kokini, 1994)

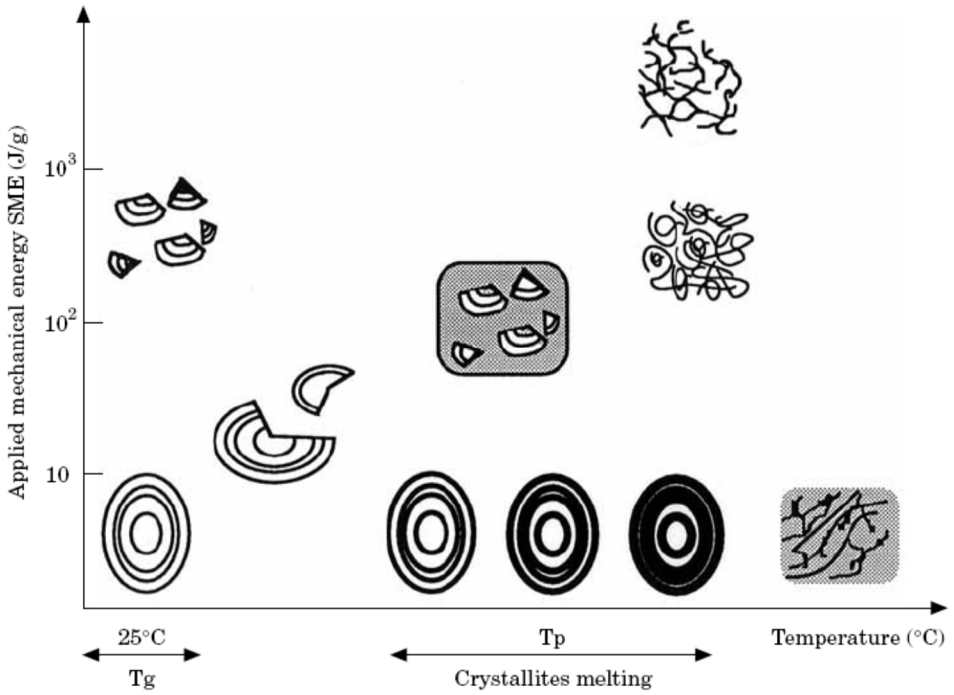

Figure 1.9 Schematic representation of starch de structuring under shear and temperature (Barron, 2001)

During extrusion, starch is processed at temperatures higher than the gelatinization temperature and is applied alongside mechanical energy input in the range

of 100 - 1000 kJ/kg (Atre, 2011). From Figure 1.9 and above data we can conclude that at the end of extrusion starch loses its original structure.

Effect of extrusion on starch influences the quality of the extruded product. Gelatinized starch loses its birefringence and its ability to imbibe water reversibly. During extrusion soluble components like amylose are leached out of starch granule increasing the viscosity of the paste/melt. Provided that there is no expulsion of water, meaning the extrusion is performed at a temperature below 100 ºC, extrudate has a texture of a firm, viscoelastic gel. However most extruded snack products, including the extrudate made in this research project, are made at temperatures greater than 100 ºC. This results in a moisture loss. Gelatinized starch has a natural tendency to precipitate and to lose moisture causing the starch portion of the extrudate to become less soluble. Amylose tends to crystallize at a faster rate compared to amylopectin. This process is termed retrogradation and is generally associated with staling of bread. In addition to high temperature, extruder exerts a high operating pressure as well; this prevents moisture in extrudate from boiling. However, as soon as extrudate leaves the extruder it is exposed to atmospheric pressure and the water instantaneously converts into superheated steam and evaporates from the extrudate. Following the ideal gas law, steam losses the temperature upon expansion. It either condenses back or escapes through the pores created in extrudate. High viscosity of the melt, due to gelatinized starch, allows some of the steam to remain entrapped inside the extrudate making it an expanded product.

1.5 Effect of Protein on extrusion

During extrusion, protein also undergoes extensive physico-chemical modification. Heat denaturation of rice proteins: albumin, globulin, and glutelin occur at: 73.3, 78.9, and 82.2 ºC; respectively (Ju, 2001). Between 73 to 85 ºC, starch and protein denature. Denatured protein has an increased hydrophobicity, which can results in stabilization of extrudate air cells. Increase in hydrophobicity of pigeonpea protein is attributed to heat and shear induced unmasking of non-polar residues from the interior of protein molecule (Okpala, 2001). Hydrophobicity of protein reaches its peak and plateaus between 85-90 ºC (Ju, 2001). Since extrusion is performed at much higher temperatures (between 120-180ºC) as compared to this (85-90 ºC) maximum possible hydrophobicity of protein and complete denaturation is achieved.

Moist heat improves the nutritional quality of pigeonpea protein compared to dry heat. This is observed by measuring available lysine content of pigeonpea. Available lysine was less in roasted (dry heat) pigeonpea compared to boiled and pressure cooked (moist heat) pigeonpea (Geervani, 1980). Since extrusion cooking is conducted at high moisture (19-23 % w.b.), superior quality of protein is expected as compared to dry heating. Extrusion cooking is also beneficial as it facilitates denaturation of antinutritional factors such as various protein inhibitors.

Pigeonpea proteins have a tendency to become lipophilic upon processing resulting into higher fat absorption capabilities. Protein denaturation enhances hydrophobicity resulting into air, fat and oil absorption (Okpala, 2001).

1.6 Effect of Lipids on extrusion

Regardless of the original state, all the fats turn into oils at extrusion conditions. All the common oils and fats have a melting point below 40 ºC. High temperature of extrusion accelerates oxidation of oils. Unsaturated oils are subjected to increasing degradation as the temperature of the extrusion is raised (Rao, 1989). As discussed, in effects of protein on extrusion, oil is adsorbed into the hydrophobic protein matrix. In addition, amylose being hydrophobic in nature adsorbs some of the lipids (Riaz, 2000). Bound lipids are unaffected by effects of lipid peroxides and thus are protected from oxidation. This enhances the shelf life of the extrudate (Karwe, 2003). Even though present at very low quantity in extruder feed, lipids have significant effects on extrusion process and sensory characteristics of extrudate.

1.7 Effect of extrusion on vitamins

Extrusion imparts many desirable effects on the main macromolecules (starch, protein, oil and crude fiber). However, its secondary effects on vitamins are destructive. Higher throughput generally ensures a higher retention of vitamins, which may be attributed to shorter residence time. Increase in specific mechanical energy (SME) results in reduction in retention of vitamins (Killeit, 1984). Extruding triticale, Beetner (1976) showed that, an increase in the die size increased the retention of vitamins; whereas, temperature had an inverse effect on their retention. In addition to the losses due to processing, extrudate has higher surface area due to expansion, which causes higher losses during storage. A study conducted by Grebaut (1983) showed that extrusion causes lower losses in vitamin C and B_1 (8.2 % and 32.2 % of the original content) content as

compared to roller drying (9.2 % and 33.2 % of the original content), but after 12 months of storage the extruded material lost more (45.8 % and 43.2 % of the original content) as compared to roller drying (37 % and 40.6 % of the original content). Vitamin A and B_2 were also studied in the same study with higher losses during the processing.

Extrusion parameters are adjusted to achieve optimal sensory quality and not for maximum retention of vitamins (Connor, 1987). Table 1.3 shows the ranges of vitamin losses on wet basis during extrusion cooking.

Table 1.3 Ranges of vitamin losses during extrusion cooking (Connor, 1987)

Fat soluble vitamins		Water soluble vitamins (continue)	
Vitamin A	12 – 88 %	Vitamin B_6	4 – 44 %
Vitamin E	7 – 86 %	Vitamin B_{12}	1 – 40 %
Water soluble vitamins		Niacin	0 – 40 %
Vitamin C	0 – 87 %	Folic acid	8 – 65 %
Vitamin B_1	6 – 62 %	Ca- pantothenate	0 – 10 %
Vitamin B_2	0 – 40 %	Biotin	3 – 26 %

1.8 Prior work on rice and pigeonpea extrusion

Extrusion of split pigeonpea with millet was conducted by Chakraborty (2011). The pigeonpea fraction in the blend was 12, 16, 20, 24 and 28 % (w.b.) with moisture content varying between 12, 15, 18, 21 and 24 % (w.b.). Other processing parameters used for optimization were: die head temperature, barrel temperature and screw speed.

In a study conducted by Kumar (2010) carrot pomace, split pigeonpea flour and rice flour were mixed at varying ratios to prepare extruder feed. The pigeonpea fraction in the mixture was maintained less than 45 % (w.b). The ratio of the components, moisture content of the feed, screw speed and die temperature were the independent variables in the RSM that was used. The effects of the independent variables on physicochemical and sensory characteristics of the finished product were observed and a model for the same was proposed.

Extrusion of pigeonpea flour supplemented with rice was conducted as masters' research project by Azman (1988). Supplementation, up to 30 % (w.b.), of pigeonpea in the formulation was studied in the absence of Basmati rice. Pigeonpea are not mentioned to be whole, and based on consumption pattern in Indonesia it is assumed to be split pigeonpea. Extrusion of pigeonpea at a ratio of higher than 50 % has not been conducted. The research hypothesis address in this thesis is can Basmati rice and whole pigeonpea be extruded with desirable textural properties?

1.9 Rationale

Traditional preparation of "dahl" has limited use due to its short shelf life. Extruded low moisture products will have significantly longer shelf-life and can be marketed as an "on the go" snack.

Preliminary experiments suggest the possibility of extruding pigeonpea at a ratio of up to 75 % (w.b.) is feasible, which was significantly higher than previous research (<50 % w.b.). In order to identify optimum conditions for the finished product quality process optimization is required.

1.10 Objectives

The overall objective of this work was to investigate effect of extrusion conditions on physicochemical properties of extrudates made from Basmati rice and whole pigeonpea flour. The specific objectives are as follows:

1. To find a feasible operating range for the extrusion of above feed mixture;
2. Optimization of the ratio of Basmati rice flour and whole pigeonpea flour in the extruder feed mixture for extrudate characteristics;
3. To study the effect of extrusion control variables on physicochemical properties of extrudates.

2. MATERIALS AND METHODS

2.1 Materials

2.1.1 Whole pigeonpea

Whole pigeonpeas were bought from a local store (Patel's Cash & Carry, 2800 State Route 27, North Brunswick Township, NJ). The brand name for the pigeonpea was "Swad®" and was kept consistent throughout the research. Composition for whole pigeonpea (as performed by an external laboratory) is provided in Table 3.1.

2.1.2 Basmati rice

Basmati rice was also bought from the same local store (i.e., Patel's Cash & Carry). The brand name for the Basmati rice was Kitchen King® Dehraduni Basmati rice. The composition for the Basmati rice (as performed by an external laboratory) is provided in Table 3.1.

2.2 Equipment

2.2.1 Mill (for making flour):

Fitzmill® (Elmhurst, Illinois, USA)

2.2.2 Particle Size Distribution Test Sieves:

Gilson Company Inc, (Lewis Center, Ohio, USA)

2.2.3 Sieve Shaker:

Tyler Ro Tap Sieve Shaker (Cleveland, Ohio, USA)

2.2.4 Moisture Analyzer:

Sartorius® MA-30 000V3 (Göttingen, Germany)

2.2.5 Planetary Mixer for blend preparation:

Kitchen Aid® Model K5-A (Kitchen Aid Division, Hobart Corporation, Troy, Ohio, USA)

2.2.6 Refrigerator for the storage of prepared flour blend:

Precision Model 815 Low Temperature Incubator (Thermo scientific, Marietta, Ohio, USA)

2.2.7 Single Screw Extruder:

Plasticorder PL-2100, Type DR-2072 C. W. Brabender Instruments, Incorporation (South Hackensack, New Jersey, USA) with poly-speed 7.5 HP motor, DC Drive, Gear Ratio 11:1

2.2.8 Incubator for drying the extrudate:

Forma Scientific® 3911Bench Model Environmental Chamber (Marietta, Ohio, USA)

2.2.9 Texture Analyzer:

Brookfield® Texture Analyzer CT3 (Middleboro, Massachusetts, USA)

2.2.10 Laboratory Blender:

Waring® Laboratory Blender (Dynamics Corporation of America, New Hartford, Connecticut USA) With a GE® 1/5 HP explosion proof motor

2.2.11 Stereopycnometer SPY-2:

Stereopycnometer SPY 2 (Quantachrome® Corp. Syosset, New York, USA)

2.2.12 Centrifuge:

International Clinical Centrifuge (Needham Heights, Massachusetts) With 1.2 AMP motor

2.2.13 Shaker:

Fisher Scientific® Nutating Mixer (Fisher Scientific, Pittsburgh, Pennsylvania, USA)

2.2.14 Chroma meter for color analysis:

Konica Minolta® Chroma M CR410 (Konica Minolta, Japan)

2.3 Methods:

2.3.1 Milling

Raw materials (Basmati rice grains or pigeonpea) was sifted manually for removal of extraneous material and fed to Fitzmill® (Figure 2.1) for flour preparation. A Fitzmill® comminutor was used to achieve a precise particle size distribution. Fitzmill® uses knife milling, which imparts optimal size reduction while adding minimal thermal input thus reduces batch to batch variation. In knife milling, the dry seeds are fed through knives rotating at high angular velocities and passed through a sieve having one millimeter diameter openings. Therefore, the obtained flour particles have diameter less than one millimeter in one orientation. Basmati rice and pigeonpea were milled on separate days to avoid intermixing of flours. The milled flour was kept in a refrigerator until used.

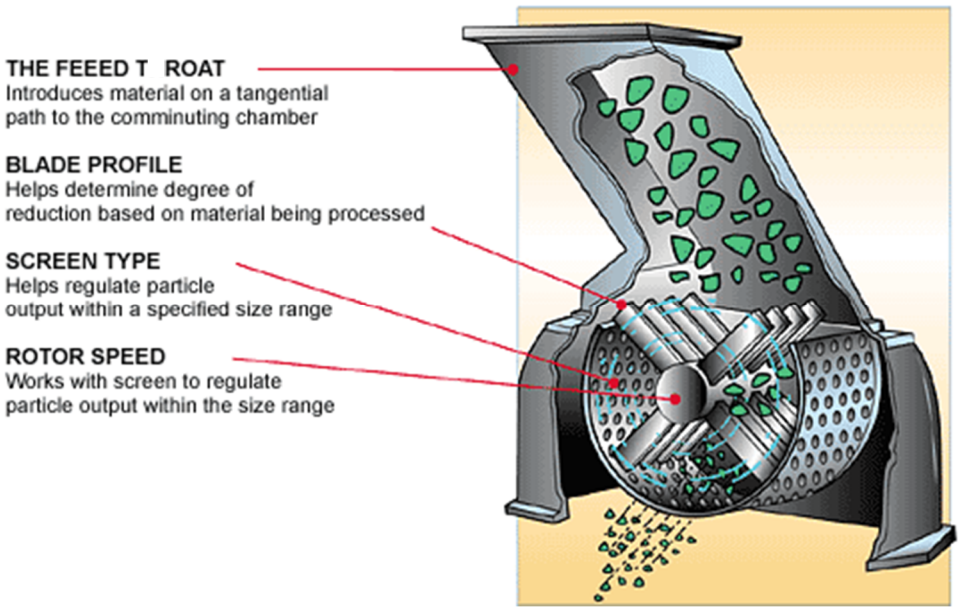

Figure 2.1: Cross sectional view of Fitzmill® comminutor

(Image courtesy of: http://www.fitzmill.com/pharmaceutical/size_reduction/theory_applications/theory_applications_pD37F.html, download date: May 25, 2011)

2.3.2 Particle Size Distribution (PSD):

PSD of Basmati rice and pigeonpea flour, was measured to evaluate its effect on extrusion process. Measurements for PSD were carried out by sieve analysis method developed by Drouzas (1988) and modified by Marousis (1990). In this method sieves were stacked in decreasing order of opening size. Order of sieve from top to bottom was mesh size 30 (600µm), 50 (300 µm), 100 (150 µm), 200 (75 µm), 325 (45 µm) and 400 (38 µm). In addition to the sieves, a lid at the top and a retainer at the bottom were added to prevent sample loss. The stack of sieves with the bottom retainer was placed in sieve shaker and a known amount of flour added to the top sieve. Lid, tapper distributor, stack holder and tapper were applied at the top. Previously, this sieve shaker was used for two, three and four minutes (Shah, 1996) and it was found that two

minutes was sufficient. For better reproducibility, the assembly was subjected to ten minutes of continuous tapping and shaking, after, which the sieves were individually weighed. The difference for each sieve from its original weight was used to calculate percentage of the retained flour. Analysis was performed in triplicates. Results were expressed as percentage of retained flour on each sieve to that of total retained flour.

2.3.3 Moisture:

In Sartorius Moisture Analyzer, approximately 1 g of sample was held at 110°C in an aluminum dish until the weight was constant. Percentage moisture was calculated by taking the difference between the weight-loss of sample and the original sample. Moisture analysis was conducted for the flour preparation immediately after extrusion and after one day of drying at 40°C in Forma Scientific® 3911 Environmental Chamber.

Moisture was expressed on wet basis. Convention used to calculate for moisture analysis was: “dry weight” - the weight after drying and “wet weight” - the weight before drying. Analysis was repeated four times to attain better accuracy. Moisture was calculated using following formula:

$$Moisture_{w\,b} = 100\ X\ \frac{wet\ weight - dry\ weight}{wet\ weight} \quad \ldots (1)$$

2.3.4 Extruder feed preparation:

In absence of a preconditioner, extruder feed from Basmati rice and pigeonpea flour was prepared a day in advance to ensure good hydration (elimination of dry core in all the particles). Even with a pre-conditioner it takes up to 3 minutes to

achieve desired water penetration and softening of starch crystals. Extruder feed preparation is required to ensure homogeneity of the extruder feed and smooth, consistent and replicable product (Ziggers, 2000)

"*Good preconditioning is half of the extruding*" Ziggers, (2000).

Flours were mixed in the ratio of as per the extrusion condition. Calculation was made based on the dry weight of the flour. The moisture content of the feed mixture, made in previous step, was measured and distilled water was added to achieve the desired moisture content. Addition of water was carried out while mixing the flour in Kitchen Aid ® K5-A planetary mixer with a KN256BBT burnished flat beater accessory. The mixer bowl was covered with a plastic sheet to avoid losses of the fines. After the required quantity of water was added to the flour mix, the mixer was operated at maximum speed (setting ten) for one minute. Flour was passed through a two millimeter sieve (US mesh ten) to prevent formation of large clumps, which causes non-uniformity in moisture distribution. The extruder feed prepared, as above, was kept overnight in a Precision® low temperature incubator at 4 °C for moisture equilibrium.

The extruder feed was analyzed for moisture content on the day of extrusion and kept at ambient temperature for at least four hours prior to extrusion. This brought the flour temperature to 25 °C.

2.3.5 Extrusion:

An extruder manufactured by C.W. Brabender was used to conduct the extrusion. It is a Plasticorder model PL 2100, single screw electrically heated air cooled unit. As shown in Figures 2.2 and 2.3, the extruder had two sections and both had

independent heating coils. The first section (near feeder) was modified from its original state by replacing the air cooling with water cooling. This modification was performed to prevent the back flow of steam generated in second section towards the hopper.

Figure 2.2 Brabender single screw extruder: Plasticorder model PL 2100

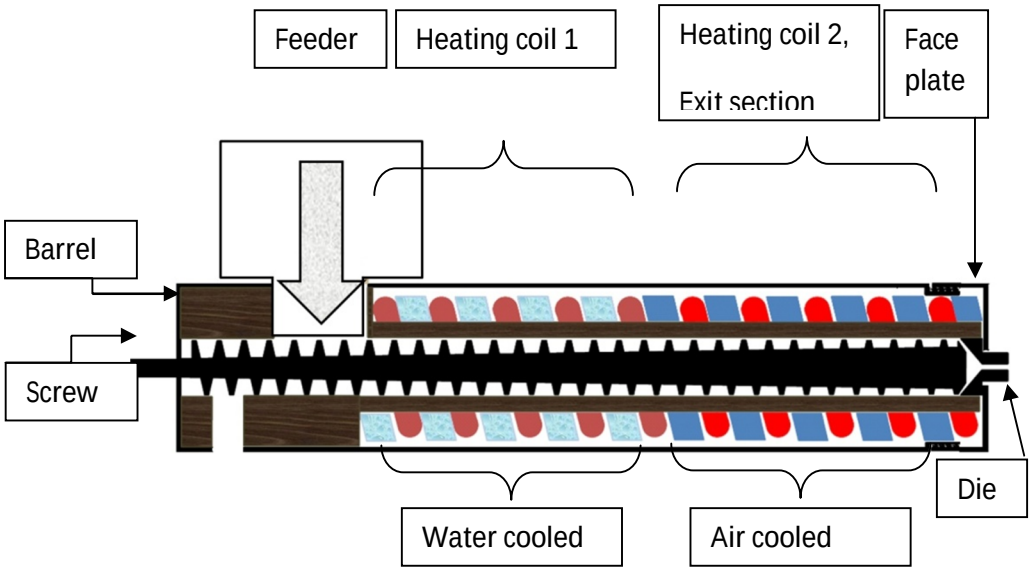

Figure 2.3 Schematic diagram of Brabender single screw extruder

The single screw used for extrusion had a tapered root diameter as shown in the Figure 2.4. It had compression ratio of 2:1, which is the ratio of volume per turn near the feed section to the same at the end. This equates to a root diameter near the feed section at 11.35 mm and near the tip at 18.8 mm. The L: D (length: diameter) ratio of the

screw was 20:1 with the helix angle of 18.29 °. The die used for extrusion had a cylindrical 3 mm hole and 5 mm in length as shown in Figure 2.5.

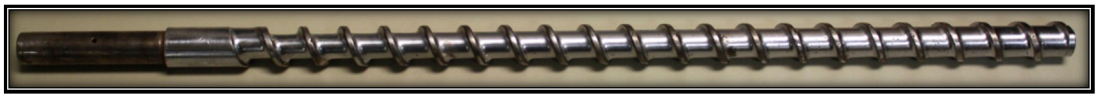

Figure 2.4 2:1 compression ratio screw used for extrusion

Figure 2.5 3 mm single hole die used for extrusion

A PID (proportional, integral and derivative) controller was used to maintain temperature of within the preset limit of less than ± 1 °C. The section near the feeder was held constant at 75 °C in order to prevent steam from next section to back track towards feeder. The maximum screw speed was 230 RPM. The range for screw speed was varied between 120 and 180 RPM, while the temperature on the exit section was between 120 °C and 180 °C. The assembly of extruder and preheating to desired set point was performed prior to start of the run. Extruder feed was added at a constant rate by hand. Steady state was validated by the extrudate flow rate, which was performed in triplicates. Samples were collected after the extruder stabilized at the required condition for at least three minutes. Flow rate (in triplicates), temperature, pressure and current drawn by the motor were recorded. At least 100 gram of extrudate was collected for analysis. Moisture content after extrusion was analyzed immediately after extrusion.

2.3.6 Drying

Extrudates were kept for 24 hours in Forma Scientific ® 3911 environmental chamber at 40 °C for drying. The environmental chamber had an internal volume of 6.1 cubic feet (≈ 0.173 m^3). This is significantly higher than the extrudate volume thus, humidity control was not found to be necessary. Moisture content after 24 hour of drying at 40 °C was analyzed. Samples not used for moisture analysis were stored in glass bottles, flushed with nitrogen gas and maintained at refrigerated storage condition.

2.3.7 Breaking strength:

Breaking strength (also known as fracture strength) is the stress when specimen fails via fracture (Degarmo, 2003). It is expressed as compressive stress that leads to structural failure of the material. Compressive stress was measured using a Brookfield Texture Analyzer CT3 (Figure 2.6). The load cell range was increased from 10 kg to 25 kg. TA-VBJ, Volodkevitch bite jaw (Figure 2.7), was used as probe due to its ability to simulate the shearing action of the front incisors as they bite through a food item similar to an extrudate. Motion of the travelling beam imitates the human “biting action”. This test was found to particularly meet the needs of extrudate analysis as its sample size requirement (1 cm^2) matches the size of the extrudate.

Figure 2.6 Brookfield Texture Analyzer (CT3) used for measuring breaking strength

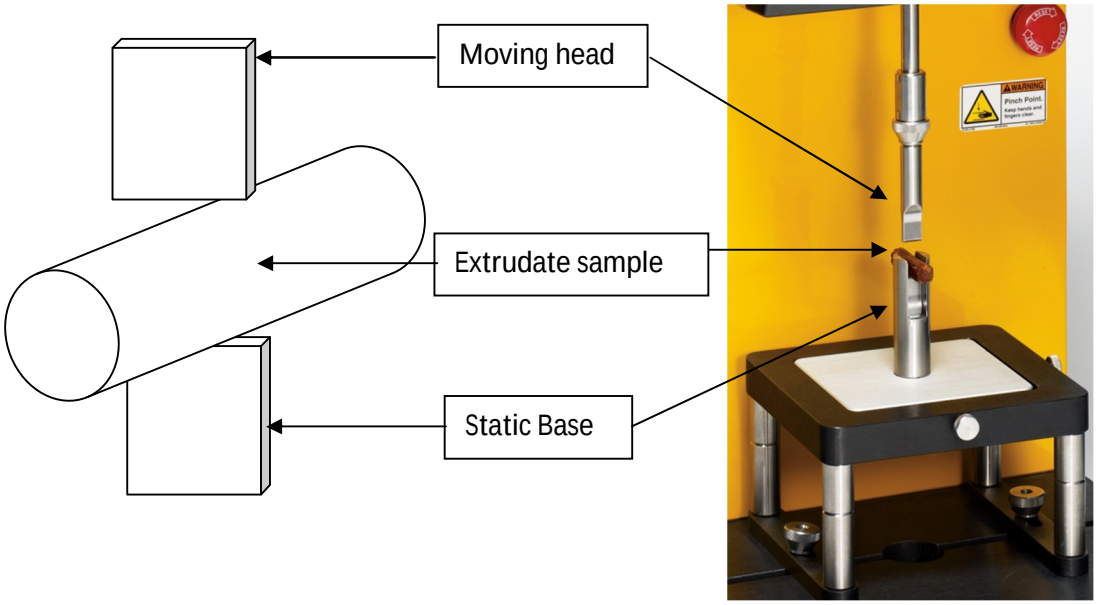

Figure 2.7 TA-VBJ (Volodkevitch bite jaws) and its schematic view

Extrudate samples were analyzed using the following procedure. A sample of extrudate was placed between Volodkecitch bite jaws as shown in Figure 2.7. The upper bite jaw was lowered at a constant rate until it reached a trigger load of 0.07 N. From then onwards the upper jaw was lowered at a constant speed of 1 mm/s till the sample was completely deformed. This evaluation utilized a single compression cycle in order to determine the shear force (peak load) and thus the breaking strength of the extrudate. An example of a chart from such analysis is illustrated in appendix.

Results were expressed as maximum shear force required to break the extrudate. Extrudate was assumed to have a perfect cylindrical shape. Cross-sectional area was calculated as $\frac{\pi D_e^2}{4}$, where D_e is the diameter of the extrudate. The analysis was repeated 10 times for reproducibility. Breaking strength was expressed in units of shear stress i.e., $\frac{force}{area}$ or $\frac{N}{m^2}$.

$$Breaking\ strength = \frac{Maximum\ load\ to\ break\ the\ extrudate\ (N)}{Area\ of\ the\ extrudate\ \frac{\pi D_e^2}{4}\ (m^2)} \quad \ldots (2)$$

2.3.8 Sectional Expansion Index (SEI):

SEI is defined as the ratio of the extrudate diameter to the orifice diameter of the die. The die diameter was measured using a digital Vernier caliper. The cross sectional area of the extrudate was measured along with breaking strength analysis in Texture analyzer CT3, which had an accuracy of 0.1 mm. SEI is a unit less dimension. Analysis was repeated 10 times for reproducibility.

$$SEI = \frac{D_e}{D_d} \quad \ldots (3)$$

Where, D_e = diameter of the extrudate (mm), and D_d = bore diameter of the die (mm).

2.3.9 Bulk Density (BD):

BD is calculated as the ratio of mass of a sample to the bulk volume. "Bulk volume" includes the voids present in the extrudate. Due to surface irregularity on extrudates, it does not closely resemble a cylindrical shape. BD was analyzed using glass beads method (Macke, 2010). 0.5 mm diameter glass beads were used. The analysis was performed in triplicates. Results were expressed as $\frac{kg}{m^3}$.

BD was calculated using following formula:

$$BD = \frac{M_{sample}}{\left(M_{wos} - (M_{ws} - M_{sample})\right) X \left(\rho_{gb}\right)} \quad \ldots (4)$$

Where,

M_{sample} = mass of the sample (kg)

M_{wos} = mass of glass beads without sample (kg)

M_{ws} = mass of glass beads with sample (kg)

ρ_{gb} = density of glass beads ($\frac{kg}{m^3}$)

2.3.10 Grinding of samples:

A Waring® laboratory blender was used to prepare fine powder of extrudates. A mortar and pestle were used as required to achieve required particle size for PD, WAI, WSI and color as explained in the subsequent sections.

2.3.11 Particle density (PD):

PD (or true density) is the ratio of mass of the powder to the volume occupied by that mass. Thus, the contribution to the volume made by pores or internal voids is subtracted for the particle density. A Quantachrome Stereopycnometer SPY -2 (Figure 2.8) was used to measure PD. It uses the Archimedes principle of fluid displacement. Dry helium, being the smallest molecule with net neutral charge (thus chemically inert), non- wetting, non-absorbent while behaving as an ideal gas, was selected as gas phase. Helium can penetrate very small void space down to 1 Å (Anonymous, 1985).

Ground flour of a known weight was placed in cell holder of known volume, Vc. Pressure was raised to approximately 17 PSI (P_1). A known volume, Va was added. And final pressure reading P_2 was taken. Calibration of the instrument was performed using reference samples of known volume, such as, a spherical steel ball and a cylindrical glass rod. Analysis was done in triplicates and results were expressed in $\frac{kg}{m^3}$.

Figure 2.8 Quantachrome stereopycnometer SPY2

(Image courtesy of: http://www.quantachrome.com/density/stereopycnom.html, download date: May 25, 2011)

The schematic diagram of stereopycnometer is shown in Figure 2.9.

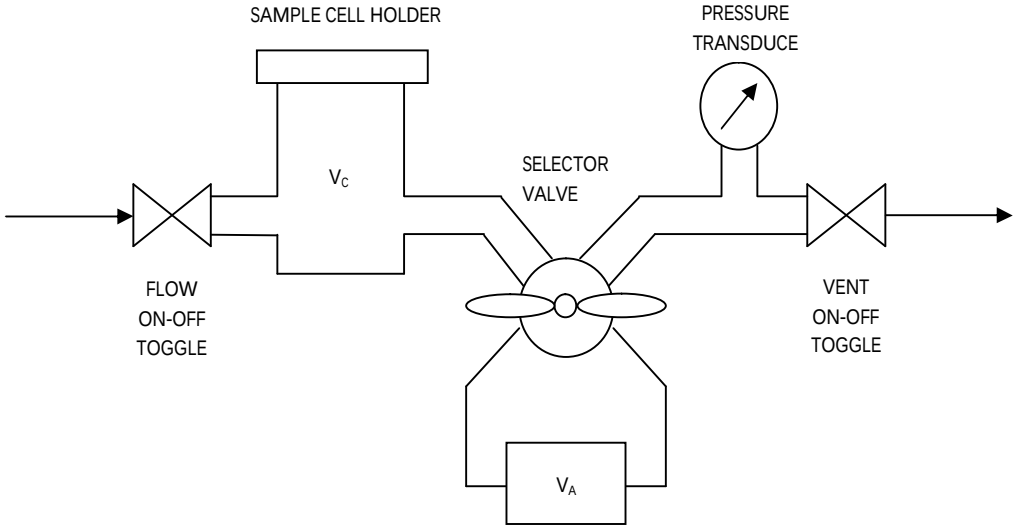

Figure 2.9 Schematic diagram of Quantachrome Stereopycnometer SPY-2

Volume of extrudate was measured using equation:

$$V_p = V_c + \frac{V_a}{1-\left(\frac{P_1}{P_2}\right)} \quad \ldots (5)$$

Where,

V_p = True volume (m^3), V_c = Sample cell holder volume (m^3), V_a = Added volume (m^3), P_1 = Pressure reading before adding V_a (psig) and P_2 = Pressure reading after adding V_a (psig)

PD was calculated using equation:

$$PD = \frac{M_p}{V_p} \quad \ldots (6)$$

Where,

M_p = Weight of sample (kg) and V_p = True volume (m^3)

2.3.12 Porosity:

Porosity is a measure expansion due to presence of void volume as compared to its original volume. It is represented as void volume as compared to total volume (sum of void and particle volume). Porosity is a unit less dimension. Porosity was calculated from BD and PD using following formula:

$$\text{Porosity} = 1 - \frac{\text{BD}}{\text{PD}} \quad \ldots (7)$$

2.3.13 Water absorption index (WAI) and water solubility index (WSI):

WAI and WSI are indicators of heat induced gelatinization and fragmentation of starch molecule, respectively. WAI shows swelling of starch granule in terms of increase in its water holding capacity. WSI shows the extent of released amylose and hydrolyzed water soluble starch products.WAI and WSI were measured using a method developed by Kite (1957) and modified to suit cereal application by Anderson (1970). 2.5 g ground sample was suspended in 25 ml distilled water at room temperature in a Corning® 50 ml centrifuge tube. Using Fisher Scientific® nutating mixer (Figure 2.10), centrifuge tubes were rotated at 20degree angle and 24 RPM for 30 minutes.

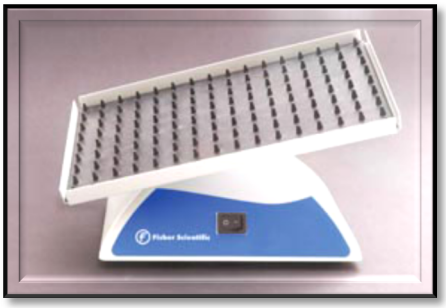

Figure 2.10 Fisher Scientific® nutating mixer

(Image courtesy of: https://fscimage.fishersci.com/images/F42400~wl.jpg, download date: May 25, 2011)

These tubes were then subjected to centrifugation at 7100 RPM for 10 minutes. Supernatant liquor was poured into an evaporating dish for moisture analysis in Sartorius® MA 30 moisture analyzer. Gels formed at bottom of centrifuge tube and were weighed and difference from dry mass in original sample of 2.5 g was calculated. All the analyses were performed in quadruplicates to balance the centrifuge. WSI was expressed as the percentage of kg water soluble matter to the original kg dry sample. WAI was calculated as kg water absorbed per kg dry sample. WAI was calculated using following formula:

$$WAI = \frac{W_f + W_w - W_s}{W_f - W_m - W_{ss}} \quad \ldots (8)$$

Where,

W_f = Mass of flour (approximately 2.5 $X10^{-3}$ kg)

W_w = Mass of distilled water (approximately 25 $X10^{-3}$ kg)

W_s = Mass of supernatant (kg)

W_m = Mass of moisture in flour (W_f X moisture fraction in flour, kg)

W_{ss} =Mass of solids in supernatant (kg)

WSI was calculated using following formula:

$$WSI = \frac{W_{ss}}{W_f - W_m} \quad \ldots (9)$$

2.3.14 Color:

The analytical method for color analysis of powder developed by Berrios, (2004) was used to measure color. Ground extrudates of maximum 0.5 mm diameter were used for color evaluation.

A Konica Minolta Chroma-Meter (CR-410) (Figure 2.11) equipped with a xenon lamp in the L*, a* and b* system. Measurement was performed at 2 °.

Figure 2.11 Konica-Minolta CR-410 colorimeter

Initial calibration was performed with a White D65 standard (Y=94.7, x = 0.3165 and y = 0.3319). Color measurements were determined by holding the sensing head at ~1 mm above the surface of the ground extrudate. L*, a* and b* values (Figure 2.12) represent Lightness (0: white and 100: black), red/green value (-80: green and +80: red) and blue/yellow value (-80: blue and +80: yellow) respectively (Wrolstad et al., 2005). Results were then converted to hue and chroma of L* C* h° expression as they are very easy to relate to earlier systems based on physical samples, such as the Munsell Color Scale (X-Rite, 1993). Measurements were performed in triplicates. Hue is an angle expressed in degrees and chroma is the distance from the center of color space (see Figure 2.12).

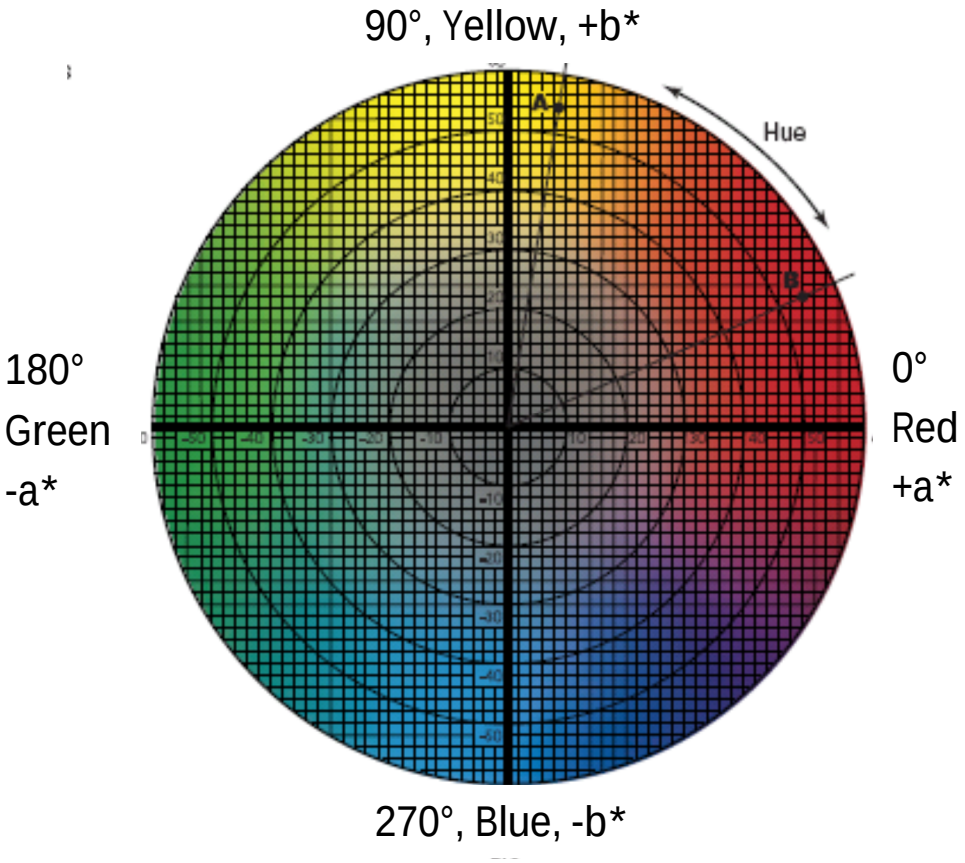

Figure 2.12 CIELAB color chart (X-Rite, 1993)

$$Hue = h° = \tan^{-1}\left(\frac{b^*}{a^*}\right) \quad \ldots (10)$$

$$Chroma = C^* = \sqrt{(a^{*2} + b^{*2})} \quad \ldots (11)$$

2.4 Statistical Analysis:

As discussed earlier viscosity of melt influenced the finished product. Viscosity is predominantly a function of temperature, moisture and shear rate (Harper, 1981). Thus the effect of temperature, moisture content, screw speed (shear rate) and ratio of Basmati rice and pigeonpea (starch content) were considered as four factors of prime importance in extrusion modeling. Response surface methodology was applied as a

'black-box method' to understand the effect of independent variables on finished product quality attributes (Akdogan, 1997). The CCD (central composite design) was used for this purpose.

"The CCD is an efficient design that is ideal for sequential experimentation and allows a reasonable amount of information for testing lack of fit while not involving an unusually large number of design points," Myers (2009).

CCD was developed by Box and Wilson (1951). 2^k designs are stepping stone for response surface methodology. For CCD analysis, axial runs and center points are added. Axial points are at a distance α from the center. Cuboidal or face centered design was chosen for the analysis, which has an α of 1 (Figure 2.12).

Four of the most significant processing conditions (factors) were chosen based on the studies conducted on similar extruder feed material. Initially a four factor three-level second order central composite (face-centered) design (CCD) was employed to extimate the effects of processing conditions on the extrudate properties.

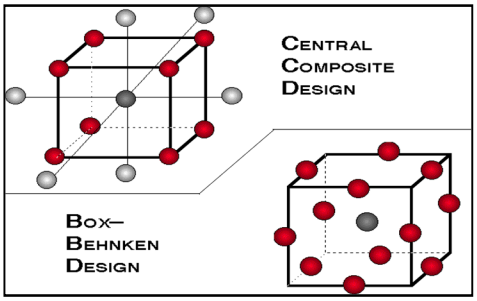

Figure 2.12 Central composite (α>1) and Box-Behnken design for 3 factors

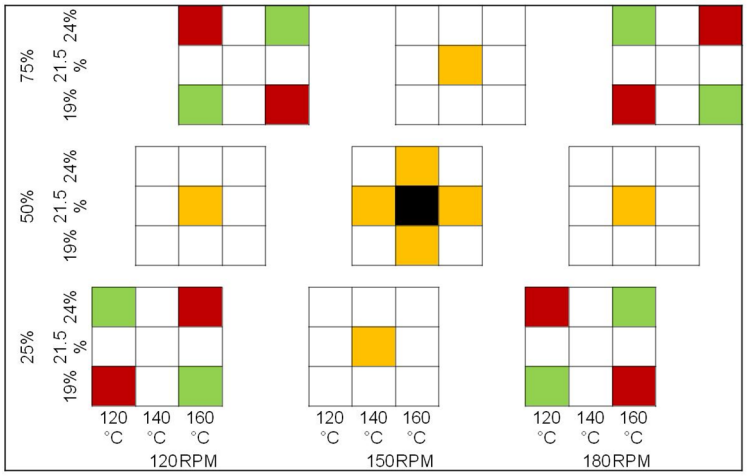

Figure 2.13 Graphical representation of set-points used for experimental design

Figure 2.13 shows graphical representation of how the set-points for experiments were selected using CCD. The point shown by the black square in the center was repeated 6 times whereas all other points were performed once. A design with 3 factors can be represented with a cube. However, for design involving 4 factors it is not possible to explain with a conventional geometric shape. Thus 3 cubes (for 3 levels of a factor) are used to graphically represent the set-points. Each set of three squares (seen vertically) describes a set-point of screw speed (i.e., 120, 150 and 180 RPM). Within each set the bottom most represent 25 % pigeonpea and remaining (i.e., 75 %) is Basmati rice. The square in middle and top represents 50 % and 75 % pigeonpea respectively. Within each square three vertical columns from left to right represent 120, 140 and 160 °C respectively. Three horizontal lines from top to bottom represent 24, 21.5 and 19 % moisture, respectively.

For response surface methodology (RSM), it is one of the assumptions that all the runs are performed under homogenous conditions, which means that except the

set-points that are intentionally changed all other processing parameters remain unchanged. Experiments involving large number or set-points (as in our case) facilitates blocking; that is, the inclusion of block effects. Blocking allows set-points to be performed in blocks (of 10 in our case). CCD provides orthogonal blocking – that is, ability to perform blocking without confounding main effects. Regression coefficients (described in analysis step) β_0, β_1, β_2 and β_3 are estimated as if the blocks were not in the experiment (Myers, 2009).

Coming back to Figure 2.13 each block is represented in red, green and yellow color. With each block center point was repeated twice. Data from the experiments were fed in to SAS 9.2 (32) statistical analysis software. Results are expressed in second-order response surface model:

$$y = \beta_0 + \sum_{i=1}^{4} \beta_i x_i + \sum_{i=1}^{4} \beta_{ii} x_i^2 + \sum \sum_{i<j=2}^{4} \beta_{ij} x_i x_j + \epsilon \quad \ldots (12)$$

After performing analysis for the aforementioned experiment, another set of run at optimum condition was performed using 3 factors 3 level Box-Behnken design (BBD) (Figure 2.12). As the name suggest BBD was introduced by Box, and Behnken, (1960). As shown in the Figure 2.12, BBD avoids usage of extreme processing conditions (corner points) and instead chooses center of each side. The ratio of pigeonpea to Basmati rice was kept constant at 50:50, because it did not show a major influence on the extrudate characteristics.

3 factors chosen for the BBD experiments were moisture content of extruder feed, temperature of exit section of extruder barrel and speed of the screw. Three levels of processing condition were coded as (-1), 0 and 1 as low, medium and high respectively. Table 2.1 shows the coded & un-coded levels for independent variables.

Table 2.1 Coded and un-coded levels for independent variables

Code	-1	0	1
Feed moisture content (% wet basis)	19	21	23
Barrel temperature (°C)	140	160	180
Screw speed (RPM)	120	150	180

Based on these levels experimental set-points were calculated as in table 2.2

Table 2.2 Three level three variables BBD in coded and un-coded variables

Run	X_1	X_2	X_3	Feed moisture (% wet basis)	Barrel temperature (°C)	Screw speed (RPM)
1	-1	-1	0	19	140	150
2	-1	1	0	19	180	150
3	1	-1	0	23	140	150
4	1	1	0	23	180	150
5	0	-1	-1	21	140	120
6	0	-1	1	21	140	180
7	0	1	-1	21	180	120
8	0	1	1	21	180	180
9	-1	0	-1	19	160	120
10	1	0	-1	23	160	120
11	-1	0	1	19	160	180
12	1	0	1	23	160	180
13	0	0	0	21	160	150
14	0	0	0	21	160	150
15	0	0	0	21	160	150

3. RESULTS AND DISCUSSION

3.1 Proximate analysis of Basmati rice flour and pigeonpea flour

Moisture and ash content was measured using Sartorius Moisture analyzer (MA 30) and a Muffle furnace. Lipid and protein analysis was provided by Leco Corporation, using Soxhlet method and Kjeldahl method, respectively. Carbohydrate content was calculated by difference.

Table 3.1 Proximate analysis of Basmati rice and pigeonpea flour (Leco corp.)

Component	Basmati rice	Pigeonpea
	Amount (% wet basis)	Amount (% wet basis)
Moisture	10.45 ± 0.05	9.23 ± 0.02
Lipids	0.87 ± 0.03	1.72 ± 0.04
Protein	8.38 ± 0.03	20.24 ± 0.02
Carbohydrate	80.18 ± 0.02	65.21 ± 0.04
Ash	0.12 ± 0.01	3.6 ± 0.02

Individual amino acid content with respect to total wet weight was measured by Leco Corporation, and was provided in Table 3.2.

Table 3.2 Amino acid analysis of Basmati rice and pigeonpea flour (Leco corp.)

Amino acids	Basmati rice (% wet basis)	Pigeonpea (% wet basis)
Aspartic acid	0.83	2.12
Threonine	0.31	0.77
Serine	0.44	0.99
Glutamic acid	1.62	4.17
Glycine	0.4	0.76
Alanine	0.49	0.87
Valine	0.55	0.97
Methionine	0.2	0.22
Isoleucine	0.36	0.8
Leucine	0.74	1.5
Tyrosine	0.14	0.39
Phenylalanine	0.48	1.85
Histidine	0.23	0.79
Lysine	0.47	1.8
Arginine	0.63	1.43
Proline	0.51	1.25
Hydroxyproline	N.D.	N.D.
Cystine	0.18	0.27
Tryptophan	0.12	0.13

N.D. - not detected

3.2 Particle size distribution of Basmati rice flour and pigeonpea flour

When a bulk solid is made up of particles of various dimensions, various terms are employed to qualitatively describe the material. The word ‘size’ is used by various researchers to represent the average dimension across the particle. A particle size distribution helps characterize typical ranges of sizes covered by terms such as ‘granular material”. Qualitative terms assigned to various particle sizes are given in Table 3.3 (Woodcock and Mason, 1987).

Table 3.3 Qualitative terms used to describe the particle size of bulk solids

Descriptive term	Typical size range	Examples
Coarse solid	5 – 100 mm	Coal, aggregates
Granular solid	0.3 – 5 mm	Rice (2 -3 mm)
Particulate solid:		
Coarse powder	100 – 300 µm	Table salt
Fine powder	10 – 100 µm	Icing sugar
Superfine powder	1 – 10 µm	Face powder
Ultrafine powder	<1 µm	Paint pigments

Particle size distribution can have effect on extrudate characteristics. Particle size of Basmati rice flour was kept as close to pigeonpea flour as possible within the block. There were variations between the blocks in terms of particle size.

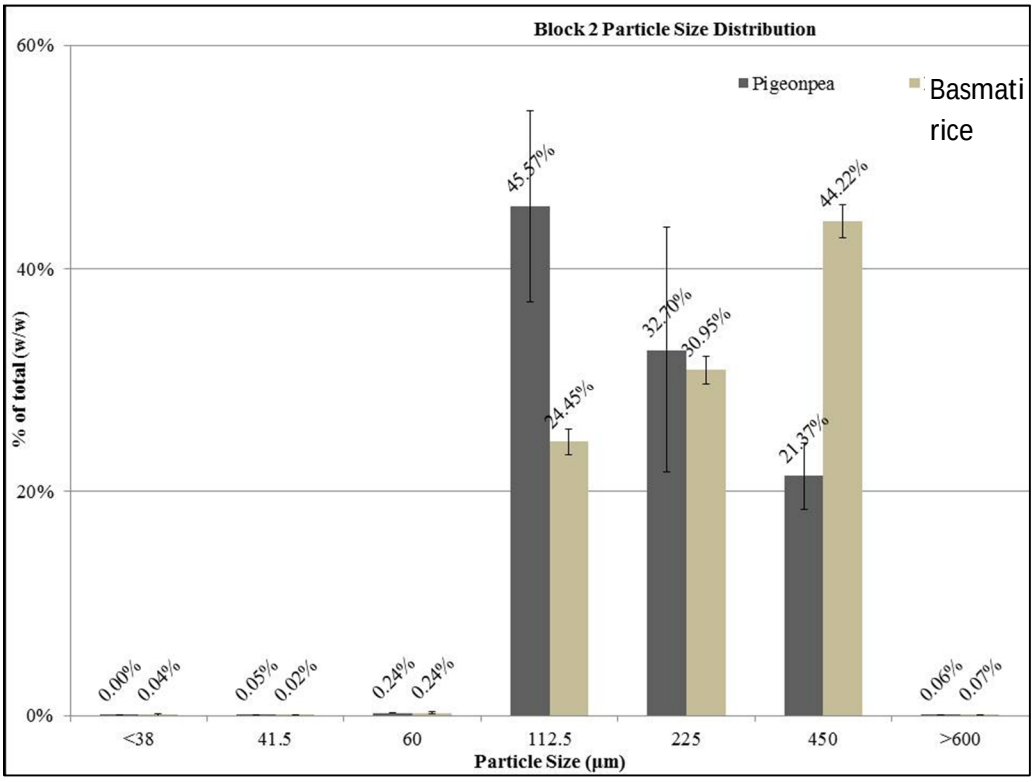

Figure 3.1 Particle size distributions of Basmati rice & pigeonpea flour for block 2

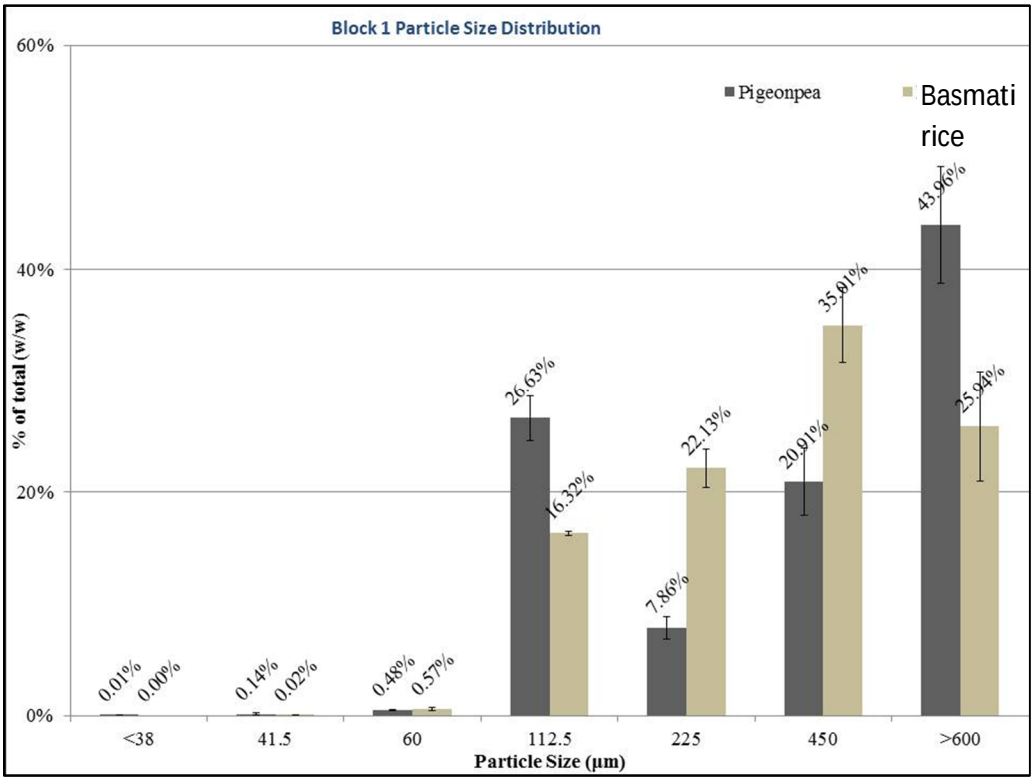

Figure 3.2 Particle size distributions of Basmati rice & pigeonpea flour for block 1

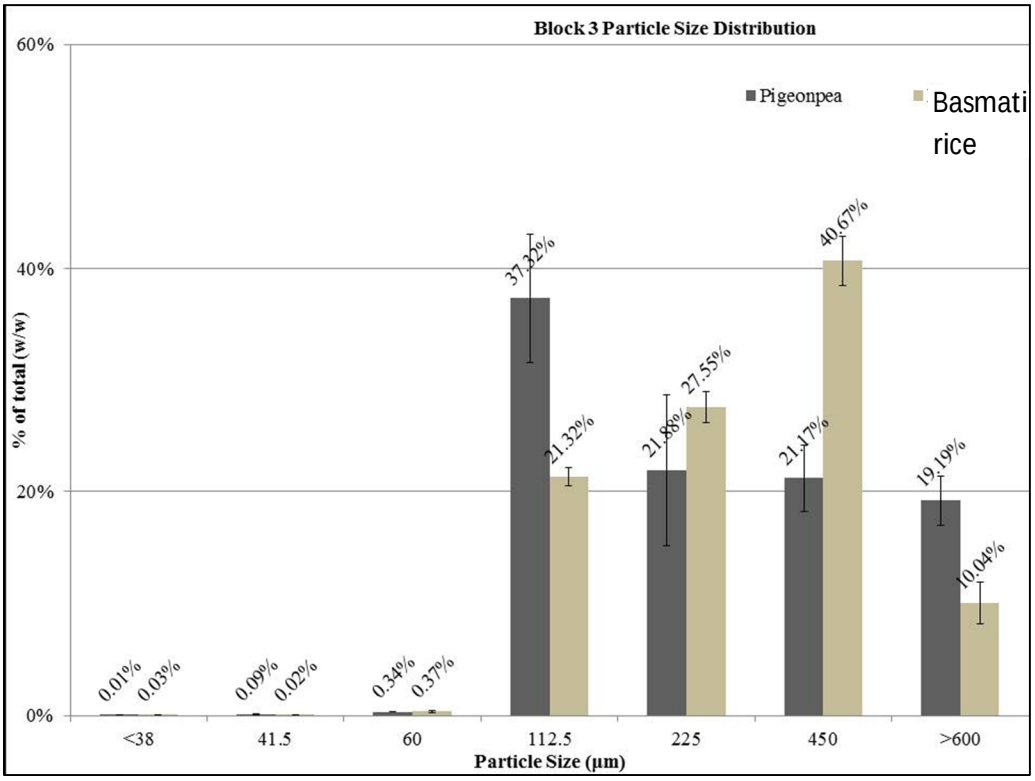

Figure 3.3 Particle size distributions of Basmati rice & pigeonpea flour for block 3

3.3 Results of four factor central composite- face centered design

A summary of results is shown in Tables 3.4, 3.5 and 3.6 for blocks 1, 2 and 3, respectively. The first 4 rows represent the operating conditions and remaining rows show the results for the same.

Table 3.4 Summary of analysis results for block 1

%PP[*1]		50	25	25	50	75	75	75	25	25	75
%Moisture		21.5	19	24	21.5	24	19	24	24	19	19
Screw speed	RPM[*2]	150	120	180	150	120	120	180	120	180	180
Temperature	°C	140	160	160	140	160	120	120	120	120	160
%Moisture	Actual	21.4	19.2	23.9	21.4	23.9	18.8	23.9	23.9	18.9	19.2
Current drawn	Ampere	7	8	4	7	2	4	2	6.2	8	1
Die pr.	MPa[*3]	11.9	20.5	7.9	12.2	3.4	7.8	2.3	12.7	24.5	1.9
Exit flow rate	kg/s	9.5	11.2	6.1	7.9	0.6	0.8	0.3	7.5	12.0	6.0
%Moisture	Initial[*4]	10.8	10.9	9.0	13.3	13.4	5.3	12.6	14.2	10.2	12.5
%Moisture	Next day	5.3	6.5	5.6	5.8	6.8	5.1	6.1	7.1	3.2	7.8
SEI		1.3	1.5	1.6	1.4	1.2	1.4	1.6	1.2	1.2	1.9
Texture	$X10^6N/m^2$	4.0	3.8	3.2	3.2	11.0	12.1	3.7	5.6	4.7	6.9
BD	$X10^3kg/m^3$	1.1	1.4	0.8	1.0	1.3	1.3	0.9	1.4	1.3	0.8
PD	$X10^3kg/m^3$	1.6	1.7	1.5	1.6	1.6	1.6	1.5	1.7	1.6	1.5
Porosity		0.3	0.2	0.5	0.4	0.2	0.2	0.4	0.2	0.2	0.5
WSI	kgss/kgds[*5]	14.3	9.2	11.4	13.6	10.6	16.9	13.9	6.2	9.4	24.2
WAI	kgwa/kgds[*6]	3.5	3.0	4.3	3.8	3.8	3.5	3.8	3.2	3.1	3.8

[*1]: Ratio of pigeonpea to Basmati rice on dry matter basis, [*2]: Revolution per minute, [*3]: Pound per square inch, [*4]: Measured immediately after extrusion, [*5]: Kg soluble solids per kg dry sample, [*6]: Kg water absorbed per kg dry sample.

Table 3.5 Summary of analysis results for block 2

%PP		50	75	25	25	75	75	50	25	75	25
%Moisture		21.5	19	19	24	24	24	21.5	24	19	19
Screw speed	RPM[*2]	150	120	120	120	120	180	150	180	180	180
Temperature	°C	140	160	120	160	120	160	140	120	120	160
%Moisture	Actual	21.4	18.8	19.2	24.3	23.9	23.9	21.5	24.3	19.3	19.0
Current drawn	Ampere	9	4	8.2	2.2	4	4	6	5	6	6.4
Die pr.	MPa	19.6	5.8	13.8	5.2	10.5	3.4	13.5	12.2	12.5	18.7
Exit flow rate	kg/s	10.9	1.58	8.3	2.5	3.2	3.2	7.9	6.5	3.9	11.3
%Moisture	Initial	14.0	10.2	8.5	15.0	12.4	12.5	14.7	12.4	11.6	11.2
%Moisture	Next day	7.9	6.1	5.0	7.0	4.5	3.6	8.4	5.3	4.4	5.3
SEI		1.5	2.4	1.4	2.0	1.3	2.0	1.9	1.6	1.5	1.8
Texture	$X10^6N/m^2$	5.2	1.3	8.1	2.5	3.1	1.1	2.5	4.6	2.3	1.8
BD	$X10^3kg/m^3$	0.9	0.4	1.2	0.7	1.1	0.6	0.8	0.9	0.6	0.7
PD	$X10^3kg/m^3$	1.5	1.5	1.5	1.5	1.6	1.5	1.6	1.6	1.5	1.6
Porosity		0.4	0.7	0.3	0.5	0.3	0.6	0.5	0.5	0.6	0.6
WSI	kg/kgds	13.8	27.8	7.3	11.6	16.0	27.7	16.4	4.4	15.5	13.1
WAI	kg/kgds	3.5	4.3	3.8	5.0	3.4	4.4	3.9	4.3	4.1	4.2

Table 3.6 Summary of analysis results for block 3

%PP		50	50	50	50	50	50	50	50	25	75
%Moisture		19	24	21.5	21.5	21.5	21.5	21.5	21.5	21.5	21.5
Screw speed	RPM[*2]	150	150	150	180	150	150	150	120	150	150
Temperature	°C	140	140	140	140	140	120	160	140	140	140
%Moisture	Actual	18.9	23.9	21.5	21.5	21.5	21.5	21.5	21.5	21.5	21.5
Current drawn	Ampere	6	7	6	4	6	10	5.5	6	5	2.5
Die pressure	MPa	4.1	11.4	9	10.3	10.3	17.5	10.3	12.4	10.3	8.7
Exit flow rate	kg/s	7.1	14.2	9.2	9.6	9.4	10.9	15.7	6.5	6.6	2.0
%Moisture	Initial	10.5	11.9	10.2	13.3	10.4	10.5	10.4	11.7	12.7	12.9
%Moisture	Next day	3.8	3.1	3.3	2.4	5.3	4.8	3.8	4.7	3.7	7.0
SEI		2.1	1.7	1.7	1.3	1.8	1.2	1.8	1.5	1.7	2.0
Texture	$X10^6N/m^2$	1.6	2.6	2.6	3.4	2.3	4.1	2.1	3.6	3.4	0.0
BD	$X10^3kg/m^3$	0.6	0.8	0.7	1.3	0.7	1.0	0.9	0.9	0.9	0.8
PD	$X10^3kg/m^3$	1.6	1.7	1.6	1.5	1.7	1.6	1.5	1.6	1.6	1.5
Porosity		0.6	0.5	0.6	0.2	0.6	0.4	0.4	0.4	0.5	0.5
WSI	kg/kgds	16.1	9.6	13.8	13.0	13.8	12.2	18.5	13.0	9.4	23.6
WAI	kg/kgds	4.1	4.4	4.2	3.3	4.5	3.4	4.4	4.3	4.8	4.3

3.4 Effect of extrusion conditions on moisture content. (CCD)

3.4.1 Moisture content on the day of extrusion (before drying). (CCD)

Moisture content of finished product was expressed on wet basis. The moisture content of extrudate was measured within an hour of extrusion to see the immediate effect of extrusion on moisture content. Moisture content ranged from 5.25 to 14.99 % (w.b.) the extrudate samples. Figure 3.4 shows the effect of moisture and barrel temperature on extrudate moisture content (while keeping ratio of pigeonpea to Basmati rice and screw speed at their average value).

The mathematical model used to predict extrudate moisture was based on the operating conditions generated. It takes into account all the factors (linear, interaction, and quadratic) and thus has higher value of correlation coefficient whereas predictive model considers only the significant factors affecting the particular product response and thus has lower value of correlation coefficient (Nidhi, 2011).

In order to define equation in mathematical formula following abbreviations are used. M: moisture content of extruder feed,

R: ratio of pigeonpea to Basmati rice,

T: barrel temperature (°C),

RPM: revolution per minute of the screw,

B_1: block 1 and

B_2: block 2.

The equations based on predictive (13) and master (14) models are given below.

$$Initial\ moisture = 11.78 + 0.74B_1 + 1.78B_2 - 0.04R + 1.24\mathrm{M} + 0.21\mathrm{RPM} + 0.41\mathrm{T} + 0.86(\mathrm{R} * \mathrm{RPM}) - 1.2(\mathrm{M} * \mathrm{RPM}) - 0.69(\mathrm{M} * \mathrm{T}) - 0.68(\mathrm{RPM} * \mathrm{T}) - 1.65\mathrm{T}^2;\ R^2 = 0.8482 \quad \ldots (13)$$

$$Initial\ moisture = 11.78 + 0.73B_1 + 1.77B_2 - 0.04R + 1.24M + 0.21RPM + 0.41T + 0.66R^2 + 0.09(R * M) + 0.86(R * RPM) + 0.38(R * T) - 0.92M^2 - 1.2 \times (M * RPM) - 0.69 \times (M * T) + 0.33RPM^2 - 0.68(RPM * T) - 1.69 \times T^2;\ R^2 = 0.8829 \quad \ldots (14)$$

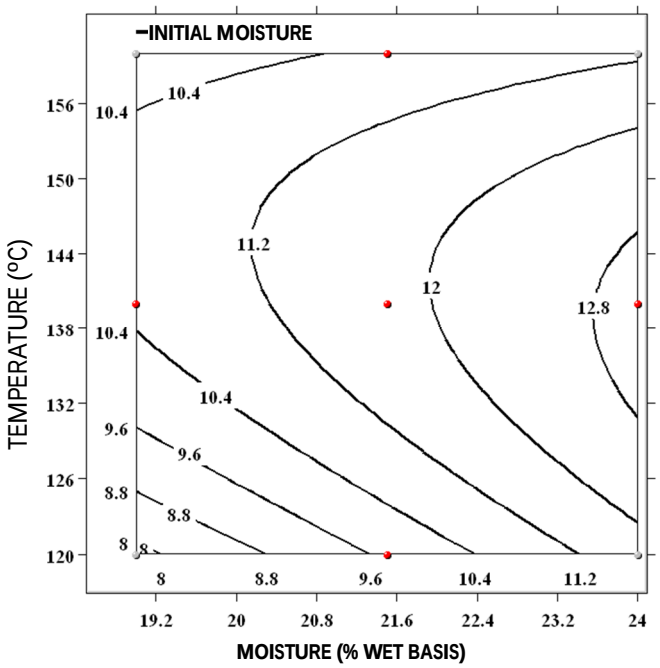

Figure 3.4 Contour plot for moisture (immediately after extrusion) of extrudate at fixed screw speed of 150 RPM and an 50:50 ratio of pigeonpea to Basmati rice.

Increased feed moisture content and screw speed results in increased extrudate moisture content. Increases in barrel temperature caused an increase in moisture content of extrudate; this can be explained by retention of moisture by the viscous melt created by gelatinized starch. Beyond 145 ºC a decrease in the moisture content was observed as barrel temperature was further increased; this can be due to the breakdown of the molecular structure of starch resulting in reduction of melt viscosity and ultimately reduction in the moisture content due to rapid flash off.

3.4.2 Moisture content of extrudate after drying at 40 ºC for 24 hours. (CCD)

The moisture content of finished product was expressed on wet basis. The moisture content of extrudate was measured after drying at 40 ºC for 24 hours to observe

the effect of extrusion on moisture content. The moisture content of extrudate ranged from 2.37 to 8.39 % (w.b.) for the extrudate samples. Figure 3.5 shows the effect of moisture and barrel temperature on extrudate moisture content (while keeping ratio of pigeonpea to Basmati rice at 50:50 and screw speed at 150 RPM). The equations based on predictive (15) and master (16) model are given below.

$$Moisture\ content\ after\ drying\ = 4.19 + 1.73B_1 + 1.54B_2 + 0.11M - 0.51RPM + 0.4T - 0.51(M * T);\ R^2 = 0.4175 \quad \ldots (15)$$

$$Moisture\ content\ after\ drying = 4.19 + 2.47B_1 + 2.28B_2 + 0.14R + 0.11M - 0.51RPM + 0.4T + 0.87R^2 - 0.47(R * M) + 0.36(R * RPM) + 0.01(R * T) - 1.02M^2 - 0.19(M * RPM) - 0.51(M * T) - 0.93RPM^2 - 0.09(RPM * T) - 0.16T^2;\ R^2 = 0.6457 \quad \ldots (16)$$

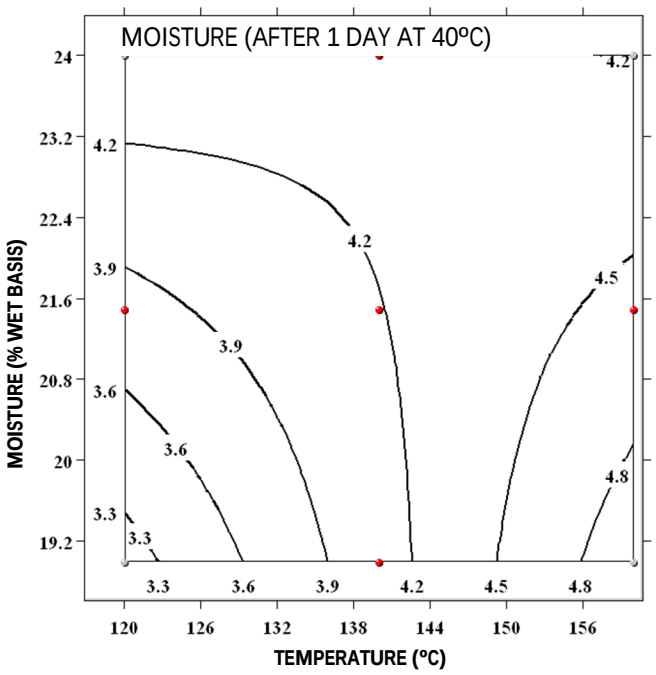

Figure 3.5 Contour plot for moisture (after 24 hours of drying at 40 ºC) of extrudates at fixed screw speed of 150 RPM and an equal ratio of pigeonpea to Basmati rice.

With an increase in screw speed there was a decrease in moisture content, which can be explained by reduction in retention time in extruder resulting in improper cooking of starch, which holds the moisture in extrudate. Increased barrel temperature resulted in increased moisture content of extrudate, this indicates that with increased barrel temperature, starch gets thoroughly more fragmented allowing it to absorb and retain more moisture. Increase or decrease in amount of pigeonpea in formulation had no significant effect in moisture content of finished product.

3.5 Effect of extrusion conditions on sectional expansion index (SEI). (CCD)

Moisture content of feed mixture and barrel temperature were the most influential factors influencing the expansion of finished product. The SEI ranged from 1.17 to 2.42. Figure 3.6 shows the effect of control variables on sectional expansion index. The equations based on predictive (17) and master (18) model are given below.

$$Sectional\ expansion\ index = 0.498 - 0.22B_1 - 0.02B_2 - 0.03M + 0.13T + 0.08M^2;\ R^2 = 0.5633 \quad \ldots (17)$$

$$Sectional\ expansion\ index = 0.498 - 0.19B_1 + 0.01B_2 + 0.04R - 0.03M + 0.03RPM + 0.13T + 0.13R^2 - 0.05(R * M) + 0.03(R * RPM) - 0.01(R * T) + 0.15M^2 + 0.06(M * RPM) - 0.04(M * T) - 0.14RPM^2 - 0.01(RPM * T) - 0.1T^2;\ R^2 = 0.8450 \quad \ldots (18)$$

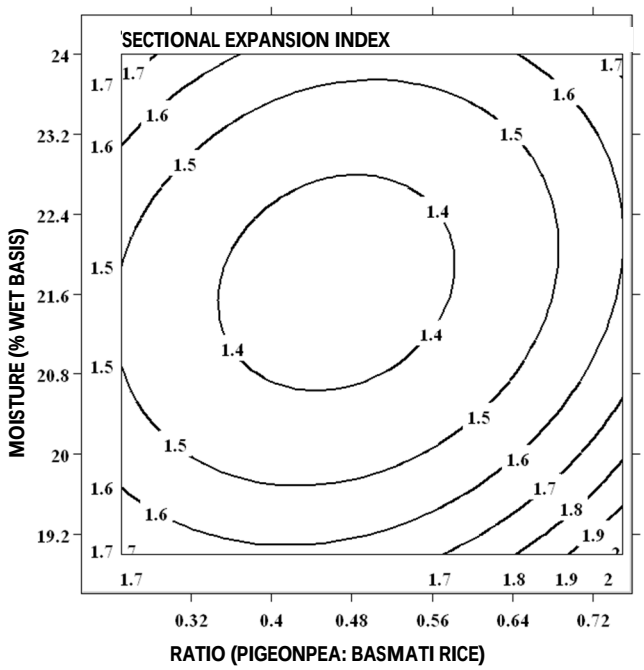

Figure 3.6 Contour plot for sectional expansion index of extrudate at fixed screw speed of 150 RPM and barrel temperature at 140 ºC.

Maximum expansion was achieved at low moisture and high pigeonpea content in the flour. An initial increase in the moisture (from 19 to 21.5 %) led to decreased expansion of the product. This may be attributed to lower friction and higher throughput of the extruder. At higher moisture content (from 21.5 to 23%), increase in the amount of moisture getting flashed off, causes higher expansion of the finished product. Basmati rice alone gives highest expansion and thus reduction in the fraction of pigeonpea in the mix gives increased expansion. As the amount of pigeonpea in the mix increases, due to presence of proteins in pigeonpea, the extent of expansion was reduced. As the content of pigeonpea increases beyond fifty percent it increases the residence time in the extruder by reducing the flow rate. This can be the primary cause of higher expansion at increased pigeonpea content in the extruder feed.

Figure 3.6 only refers to the factors (i.e., moisture content and ratio) that are most influential to the SEI of the extrudate. In order to represent all the data generated through the CCD experiments, a grid of contour plots was required to be drawn as shown in Figure 3.7

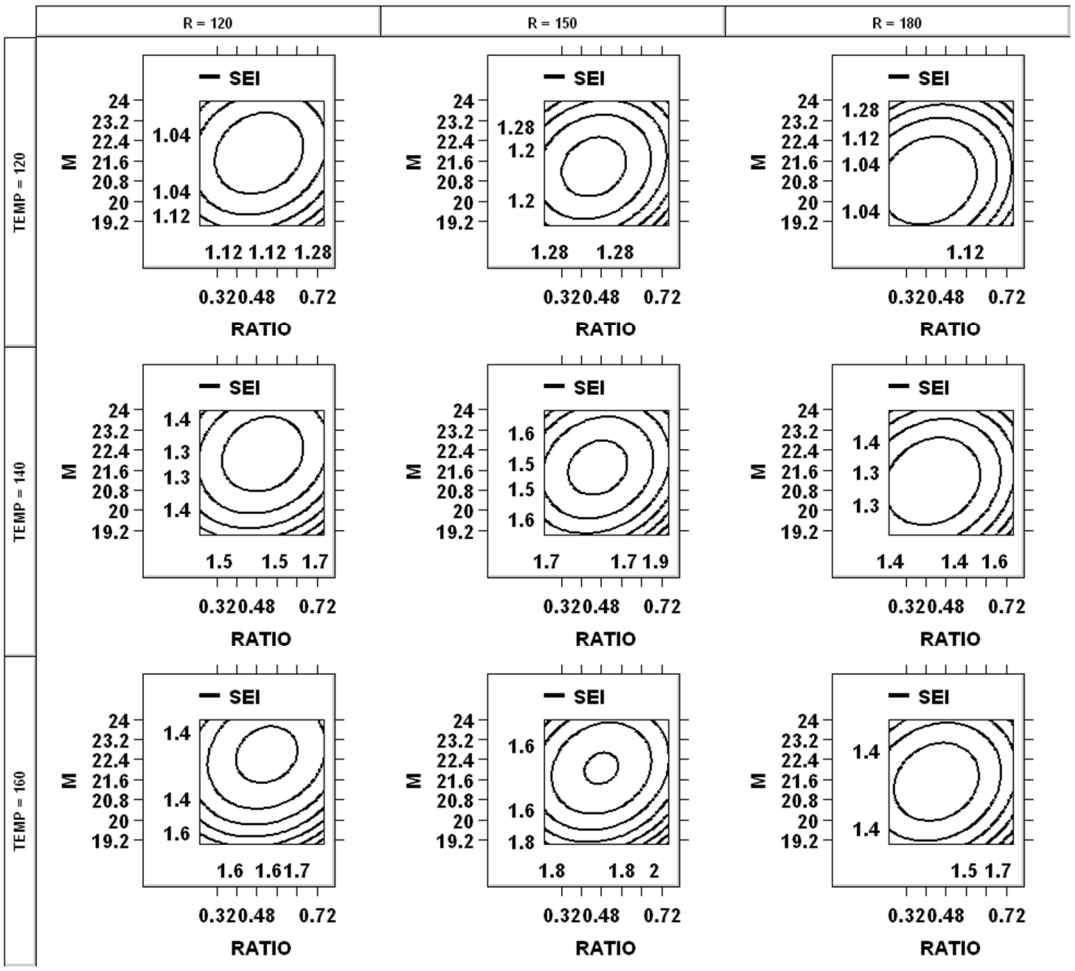

Figure 3.7 Grid of contour plot summarizing the effect of four independent variables on sectional expansion index of extrudate.

However, this plot still does not show the effect of blocks. As mentioned earlier each block has a different particle size distribution and with a minor variation between

the flours used for each block it was assumed that the blocking would not have a significant effect on the finished product.

As the master model and the predictive model state that blocking was a major effect in finished product expansion, it means that particle size distribution had a direct influence on the expansion. This can be explained by the difference in flow characteristics of flour of different particle size.

3.6 Effect of extrusion conditions on bulk density. (CCD)

Moisture content of feed mixture, barrel temperature and screw speed were the most influential factors in determining the expansion of finished product. The range of bulk density was from 0.42 to 1.40 X 10^3 $\frac{kg}{m^3}$. Figure 3.8 shows the effect of control variables on bulk density. The equations based on predictive (19) and master (20) model are given below.

$$Bulk\ density\ = 0.84 + 0.27B_1 - 0.08B_2 - 0.1RPM - 0.11T;\ R^2 = 0.5568 \quad \ldots (19)$$

$$Bulk\ density\ = 0.84 + 0.25B_1 - 0.1B_2 - 0.08R - 0.1RPM - 0.11T - 0.07R^2 + 0.1(R * M) - 0.01(R * RPM) + 0.02(R * T) - 0.14M^2 - 0.02(M * RPM) + 0.01(M * T) + 0.2RPM^2 + 0.02(RPM * T) + 0.05T^2;\ R^2 = 0.7790 \quad \ldots (20)$$

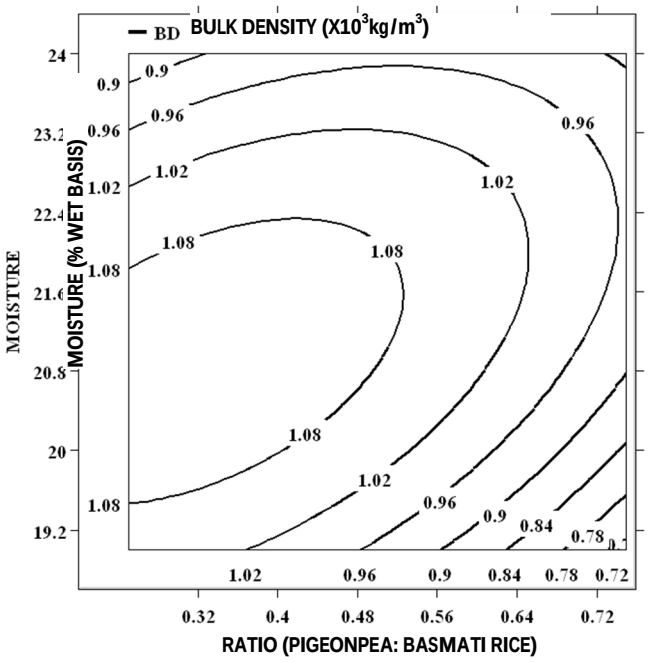

Figure 3.8 Contour plot for bulk density of extrudate at fixed screw speed of 150 RPM and barrel temperature at 140 ºC.

An increase in temperature caused a decrease in the extrudate bulk density. This may be attributed to over cooking of starch resulting in lower melt viscosity and thus reduced air pocket holding capacity. Increases in screw speed caused a decrease in bulk density, which may be due to reduction in holding time and reduced expansion of finished product. The effect of moisture content in the product and amount of pigeonpea in the extruder feed were not profound on the bulk density of the extrudate. Block 2 had a lower bulk density as compared to other block, which shows that particle size distribution has a significant effect on bulk density. Since it was an important factor for expansion of extrudate the results of expansion can be inversely correlated with bulk density.

3.7 Effect of extrusion conditions on particle density. (CCD)

All four independent factors had an effect on particle density. The range of particle density was from 1.48 to 1.67 X $10^3 \frac{kg}{m^3}$. Figure 3.9 shows the effect of control variables on particle density. The equations based on predictive (21) and master (22) model are given below.

$$Particle\ density = 1.58 + 0.01B_1 - 0.01B_2 - 0.02R + 0.01M - 0.02RPM - 0.01T - 0.03R^2 + 0.06M^2 - 0.04RPM^2 - 0.003T^2;\ R^2 = 0.39 \quad \ldots (21)$$

$$Particle\ density = 1.58 + 0.01B_1 - 0.01B_2 - 0.02R + 0.01M - 0.02RPM - 0.01T - 0.03R^2 + 0.01(R*M) - 0.01(R*RPM) + 0.01(R*T) + 0.06M^2 - 0.01(M*RPM) - 0.02(M*T) - 0.04RPM^2 - 0.002(RPM*T) - 0.003T^2;\ R^2 = 0.54 \quad \ldots (22)$$

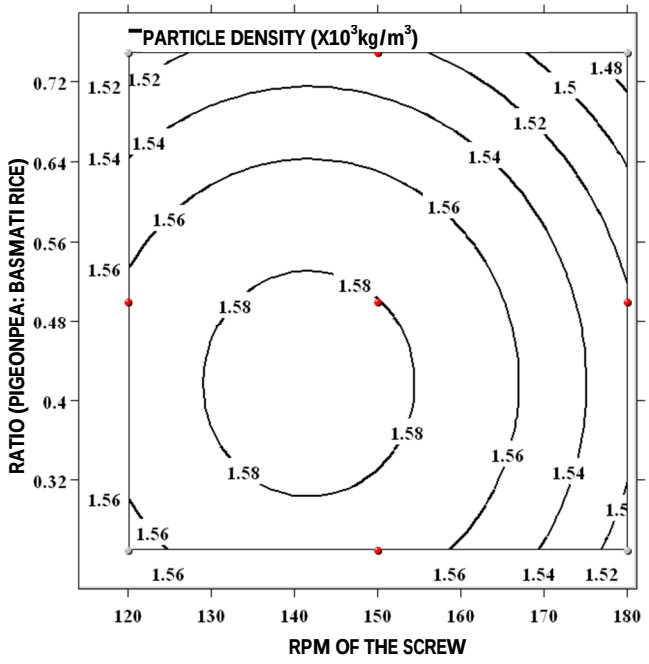

Figure 3.9 Contour plot for particle density of extrudate at fixed moisture content of 21.5 % on wet basis and barrel temperature at 140 ºC.

3.8 Effect of extrusion conditions on water solubility index. (CCD)

Ratio of pigeonpea to Basmati rice in the blend and barrel temperature were found to be the influential factors for water solubility index. The range of water solubility index varied from 4.40 to 27.80 $\frac{kgss}{kgds}$. Figure 3.10 shows the effect of control variables on water solubility index. Predictive (23) and master (24) model equations are given below.

$$Water\ solubility\ index\ = 14.288 - 0.57B_1 + 1.06B_2 + 6.31R + 3.98T;\ R^2 = 0.8824 \quad \ldots (23)$$

$$Water\ solubility\ index\ = 14.288 - 0.25B_1 + 0.78B_2 + 6.28R - 0.51M - 0.27RPM + 3.94T + 2.18R^2 + 0.15(R * M) - 0.46(R * RPM) + 1.46(R * T) - 1.45M^2 - 0.08(M * RPM) + 0.56(M * T) - 1.31RPM^2 + 0.43(RPM * T) + 1.03\,T^2;\ R^2 = 0.9647 \quad \ldots (24)$$

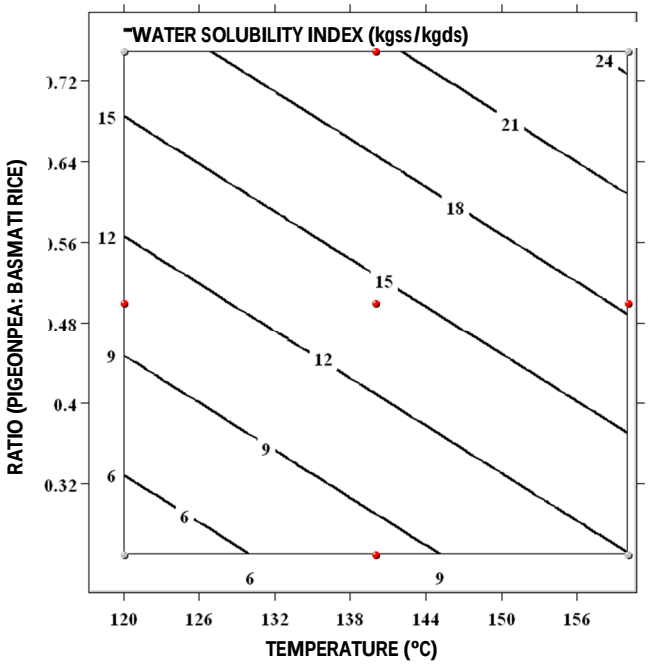

Figure 3.10 Contour plot for water solubility index of extrudate at fixed moisture content of 21.5 % on wet basis and Screw Speed at 150 RPM.

The results for water solubility index have a higher value of R^2 as compared to other effects. With increase in temperature starch granules swells and liberates water soluble amylose in the surrounding liquid. This explains the increase in water solubility index with an increase in barrel temperature. Pigeonpea has a significantly higher amount of minerals as compared to Basmati rice. This justifies the increase in water solubility index with increase in the content of pigeonpea in the extruder feed mixture. Moisture and screw speed did not show any significant effect on the water solubility index.

3.9 Effect of extrusion conditions on water absorption index. (CCD)

Barrel temperature was found to be the single most influential factors for water absorption index. The range of water absorption index was from 3.01 to 4.99 $\frac{kgwa}{kgds}$. Figure 3.10 shows the effect of control variables on water absorption index. The equations based on predictive (25) and master (26) model are given below.

$$Water\ absorption\ index\ = 0.39 - 0.59B_1 - 0.09B_2 + 0.24T;\ R^2 = 0.4242 \quad \ldots (25)$$

$$Water\ absorption\ index\ = 0.39 - 0.72B_1 - 0.21B_2 - 0.02R + 0.14M + 0.06RPM + 0.24T + 0.49R^2 - 0.2(R * M) + 0.01(R * RPM) - 0.05(R * T) + 0.17M^2 + 0.04(M * RPM) + 0.11(M * T) - 0.27RPM^2 - 0.05(RPM * T) - 0.16T^2;\ R^2 = 0.7256 \quad \ldots (26)$$

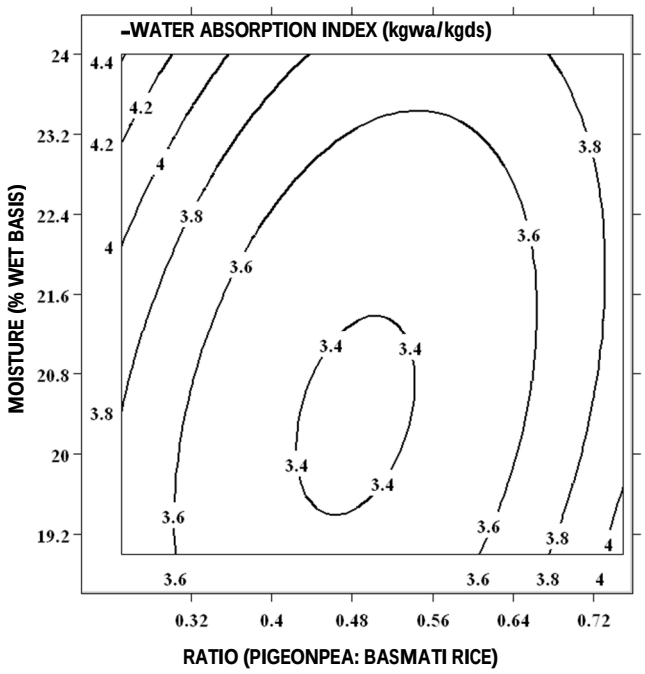

Figure 3.11 Contour plot for water absorption index of extrudate at fixed barrel temperature of 140 ºC and Screw Speed at 150 RPM.

Water absorption index has a very narrow range of results. Inherent variation within the sample was wide enough to reduce the quality (in terms of R^2) of the resulting model. Barrel temperature was found to have the direct correlation with the water absorption index. An increase in temperature causes starch expansion; this allows the crystalline regions of starch to become available to absorb more moisture. All other parameters had little or no effect on water absorption index.

3.10 Effect of extrusion conditions on breaking strength. (CCD)

Barrel temperature and ratio of pigeonpea to Basmati rice were found to be the most influential factors for breaking strength. The range of breaking strength was from

0.02 to 12.10 X 10^6 $\frac{N}{m^2}$. Figure 3.10 shows the effect of control variables on breaking strength. The equations based on predictive (27) and master (28) model are given below.

$$Breaking\ strength\ = 2.56 + 1.13B_1 + 0.53B_2 - 1.88R - 1.94T;\ R^2 = 0.6781 \quad \ldots (27)$$

$$Breaking\ strength\ = 2.56 + 1.19B_1 + 1.43B_2 - 1.32R + 0.26M - 0.19RPM - 1.36T - 0.73R^2 - 0.61(R * M) - 0.62(R * RPM) + 0.72(R * T) - 0.35M^2 + 1.41(M * RPM) + 1.09RPM^2 + 0.69T^2;\ R^2 = 0.9010 \quad \ldots (28)$$

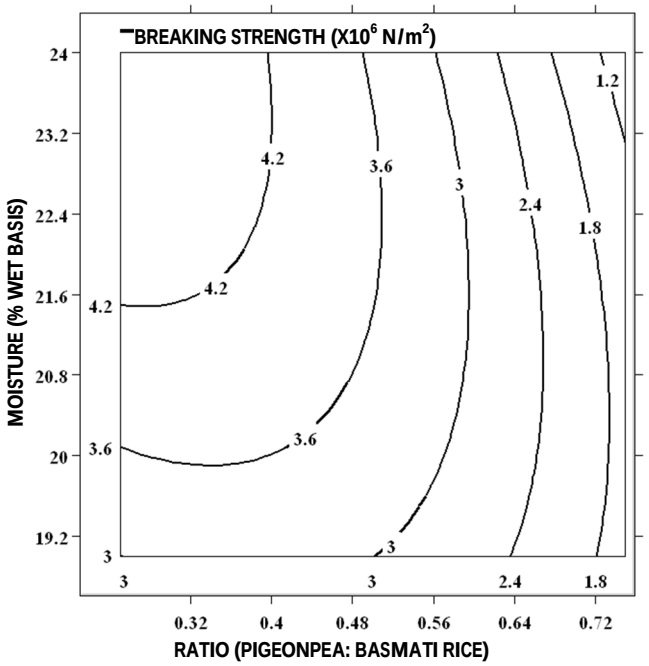

Figure 3.12 Contour plot for breaking strength of extrudate at fixed barrel temperature of 140 ºC and Screw Speed at 150 RPM.

Ratio of pigeonpea to Basmati rice in the feed had an inverse effect on breaking strength of the extrudate. Higher amount of protein in pigeonpea allowed extrudate to become brittle and crumble while testing. Whereas increase in Basmati rice allowed

higher amount of starch in the extrudate, which means that the gelatinized starch would give a gummy texture and would not crumble between the Volodkevitch bite jaws. Increased temperature caused a decreased breaking strength of extrudate. As seen earlier, increased temperature decreased the bulk density of extrudate and increases the expansion of the extrudate. This makes extrudate more brittle resulting into lower breaking strength.

3.11 Residual Plots for CCD

To examine that those fitted models provide an adequate approximation to the true system and ensure that none of the least squares regression assumptions are violated residual analysis is performed (Myers, 2009).

Model adequacy was judged by residuals from the least squares fit, defined by:

$e_i = y_i - Y_i'$, where y_i was the experimental mean and Y_i' was the predicted response. As seen in the following diagram the residuals are scattered randomly on the display. This implies that the original observations are constant for all values of y.

A funnel shaped pattern in residual plot indicates the requirement to perform transformation of the response variable. In general any non-random pattern on these plots would indicate model inadequacy (Myers, 2009).

A check for lack of fit in this manner was performed for each individual physicochemical characteristic for extrudate. Figure 3.13 to 3.18 shows the residual plot for: sectional expansion index, bulk density, particle density, water solubility index, water absorption index and breaking strength.

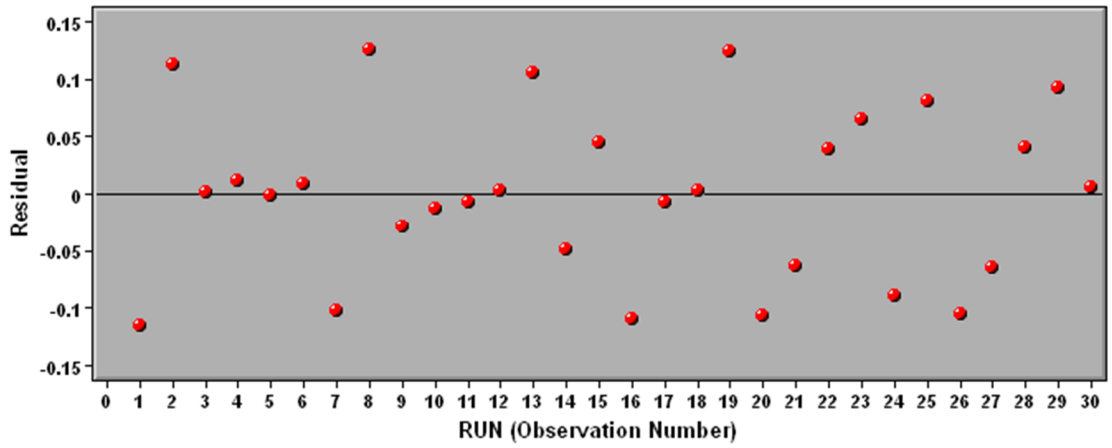

Figure 3.13 Residual plot for sectional expansion index of the extrudate. (CCD)

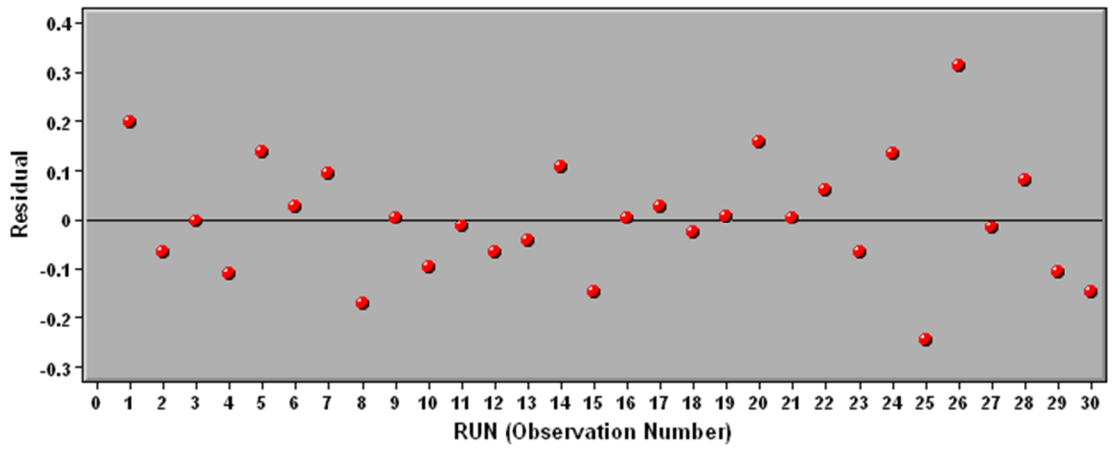

Figure 3.14 Residual plot for bulk density of the extrudate. (CCD)

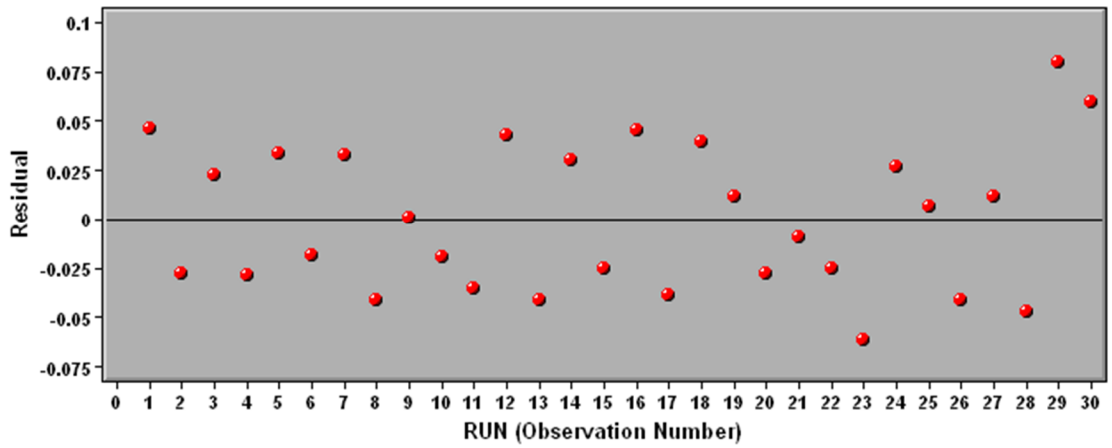

Figure 3.15 Residual plot for particle density of the extrudate. (CCD)

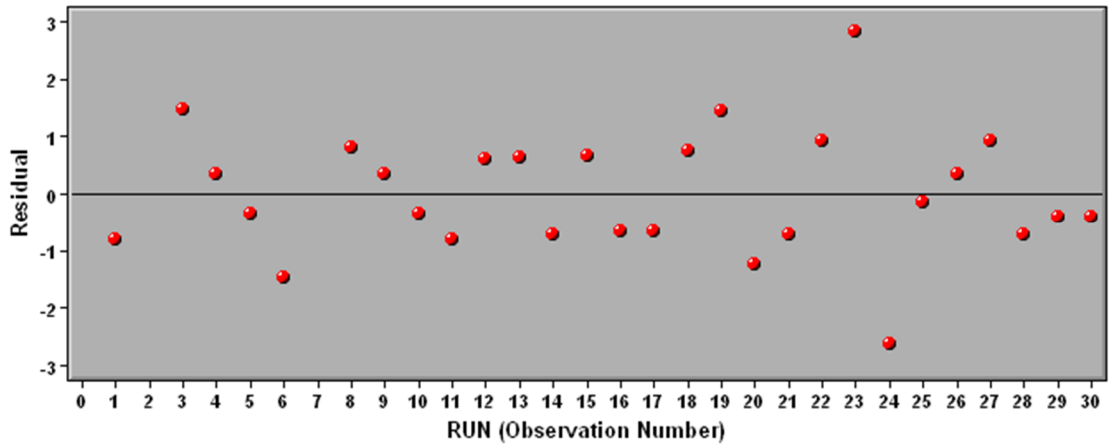

Figure 3.16 Residual plot for water solubility index of the extrudate. (CCD)

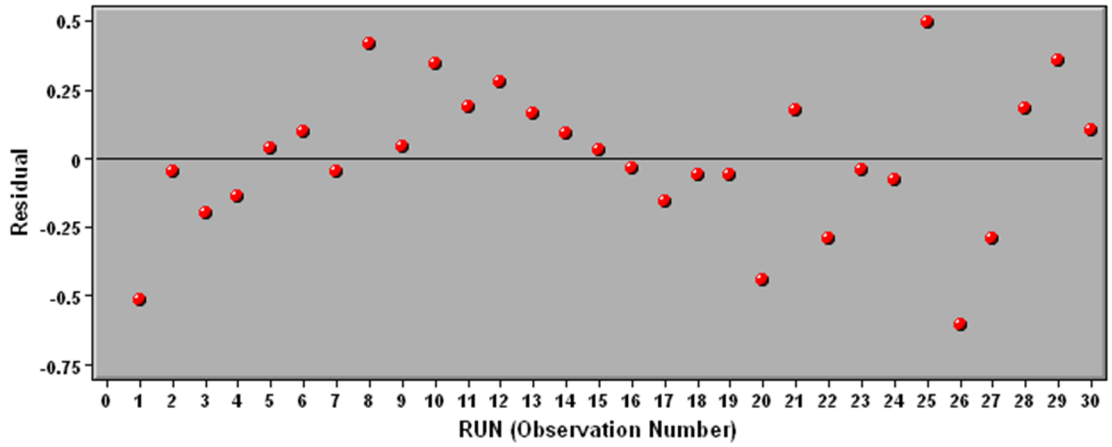

Figure 3.17 Residual plot for water absorption index of the extrudate. (CCD)

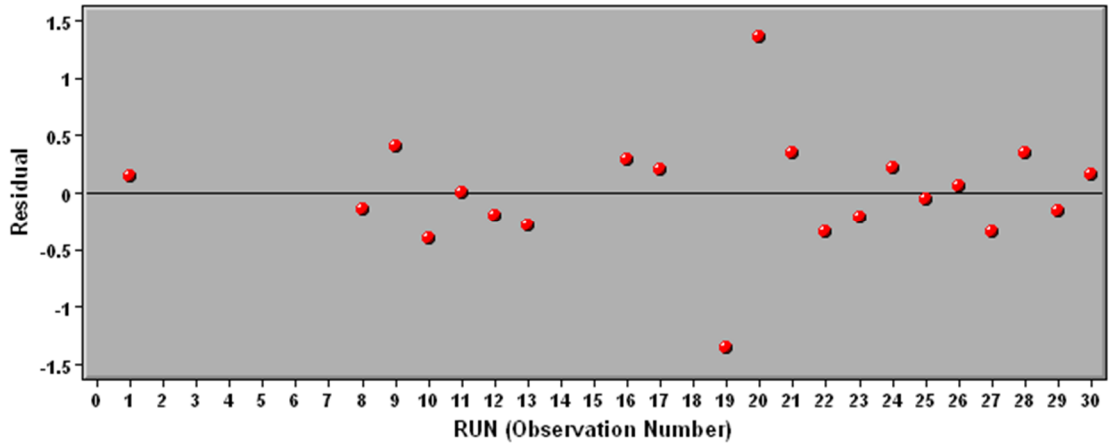

Figure 3.18 Residual plot for breaking strength of the extrudate. (CCD)

From the analysis of the results for the experiments based on the central composite design (face centered), it was found that 50:50 ratio of pigeonpea flour: Basmati rice was optimum. It gave nutritional benefits of addition of pigeonpea in the formulation while keeping acceptable processability of the mixture. Thus it was kept as a constant in second set of experiments. Water solubility index had a linear equation. Water absorption index was influenced by particle size distribution and thus would need a separate analysis. Particle density was not affected significantly by the operation parameters. These analyses were omitted in the final design. Hue and chroma were added to evaluate the effect of processing parameters on extrudate color. Box-Behnken design was used to analyze the effect of Moisture content of extruder feed, Barrel temperature and Screw speed on extrudate properties. Properties measured were: sectional expansion index, breaking strength, hue and chroma. In addition distance where the extrudate breaks was also measured and modeled.

3.12 Effect of extrusion conditions on sectional expansion index. (BBD)

Barrel temperature and moisture content of the extruder feed were found to be the most influential factors for breaking strength. The range of sectional expansion index was from 1.56 to 2.00. Figure 3.19 shows the effect of control variables on breaking strength. The equations based on predictive (29) and master (30) model are given below.

$$Sectional\ expansion\ index\ = 1.78 + 0.08M + 0.07T;\ R^2 = 0.4654 \quad \ldots (29)$$

$$Sectional\ expansion\ index\ = 1.79 + 0.08M + 0.07T + 0.01RPM - 0.03M^2 - 0.05(M * T) - 0.01(M * RPM) - 0.09T^2 - 0.05(T * RPM) - 0.09RPM^2;\ R^2 = 0.8581 \quad \ldots (30)$$

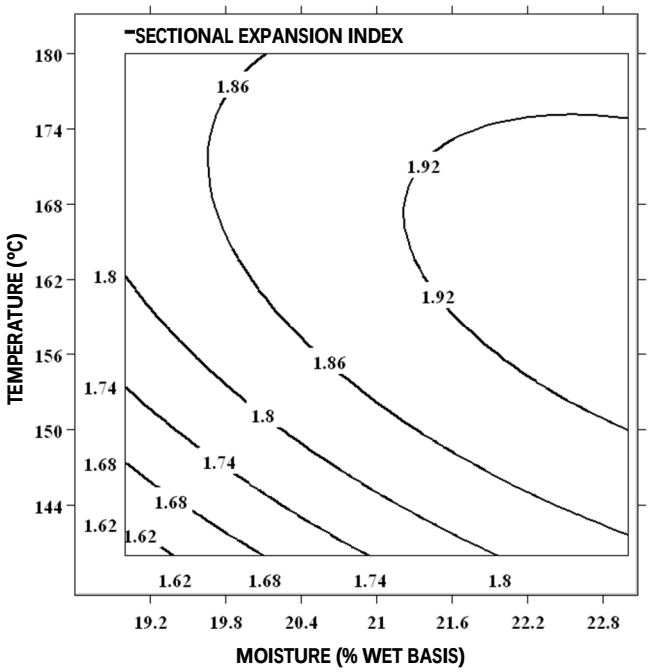

Figure 3.19 Contour plot for sectional expansion index of extrudate at constant screw speed of 150 RPM.

Moisture and temperature had a directly proportional effect on expansion of the extrudate. As the amount of moisture increased the quantity of moisture that flashes off increased thus it results into an expanded product. Temperature provides latent and sensible heat to the moisture and increase in temperature provides higher enthalpy to moisture causing an expanded product. In case of temperature beyond 168 ºC inverse correlation was noted. This can be due to over cooking of starch resulting in lower viscosity of melt, which ultimately allows the steam to escape and not attain the maximum possible expansion. The screw speed did not have significant effect on the expansion of the extrudate.

3.13 Effect of extrusion conditions on breaking strength. (BBD)

Moisture content of the extruder feed, screw speed and interaction product thereof were found to be the influential factors for breaking strength. The range of breaking strength was from 7.68X10^5 to 1.55X10^6 $\frac{N}{m^2}$. Figure 3.20 shows the effect of control variables on breaking distance. The equations based on predictive (31) and master (32) model are given below.

$$Breaking\ strength = 1223761 - 11562.1M - 72989RPM - 4165(M * RPM);\ R^2 = 0.2473 \quad \ldots (31)$$

$$Breaking\ strength = 1223761 - 11562M - 84934T - 72989RPM - 35583M^2 + 207747(M * T) - 4165(M * RPM) + 245067T^2 + 35403(T * RPM) + 39777RPM^2;\ R^2 = 0.7843 \quad \ldots (32)$$

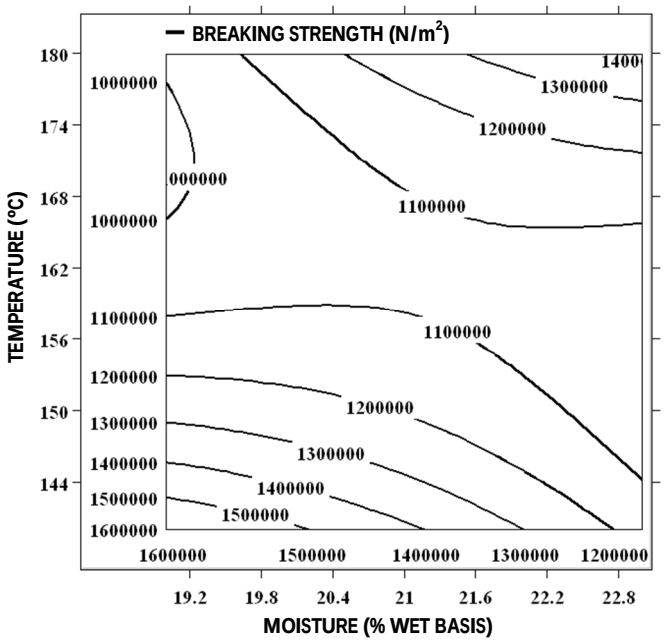

Figure 3.20 Contour plot for breaking strength of extrudate (screw speed at 150 RPM)

R^2 of the breaking strength in this set of experiment (0.63) was far lower than that of the previous set of experiments (0.90). In contradiction to previous results, temperature did not show significant effect on breaking strength of the extrudate. Increase in the screw speed resulted in decrease in breaking strength, this may be attributed to lower residence time in the extruder due to higher screw speed. Moisture also had a similar inverse correlation; however its effect was not as pronounced as screw speed.

3.14 Effect of extrusion conditions on breaking distance. (BBD)

All three independent variables and squared term of them were found to be the influential factors for breaking distance. The range of breaking strength was from 7.36 to 13.28 % of extrudate diameter. Figure 3.21 shows the effect of control variables on breaking distance of the extrudate. The equations based on predictive (33) and master (34) model are given below.

$$Breaking\ distance = 0.01 + 0.001M - 0.003T + 0.0001RPM + 0.003M^2 + 0.004RPM^2;\ R^2 = 0.8193 \quad \ldots (33)$$

$$Breaking\ distance = 0.001 + 0.001M - 0.003T + 0.0001RPM + 0.003M^2 + 0.0006(M * T) + 0.001(M * RPM) + 0.002T^2 - 0.0005(T * RPM) + 0.005RPM^2;\ R^2 = 0.9454 \quad \ldots (34)$$

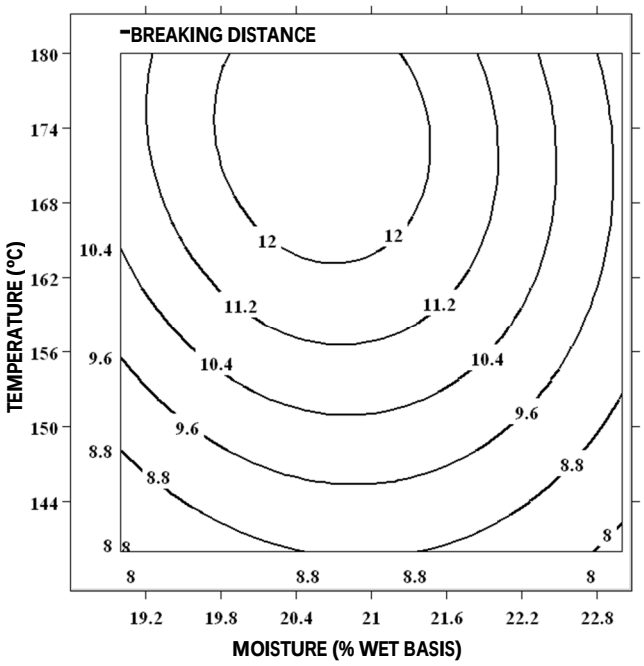

Figure 3.21 Contour plot for breaking distance of extrudate (screw speed at 150RPM)

Since we could not get a good/ acceptable correlation, new approach to statistical analysis was applied by measuring minimum distance where extrudate can be split into two separate pieces by Volodkevitch bite jaws. This represents how much the molar teeth would have to travel before extrudate breaks into two. It was observed that increase in temperature helps molecular rearrangement in extrudate allowing it to withstand for a longer bite before breaking. Increase of moisture content from 19 to 21 % enhances the breaking distance. Beyond 21 % reduces the breaking distance; this may be due to higher expansion of extrudate weakening the strength of the extrudate.

3.15 Effect of extrusion conditions on hue. (BBD)

Screw speed was found to be the influential factors for hue. The range of hue was from 80.33 to 85.54º. Figure 3.22 shows the effect of control variables on hue of the extrudate. The equations based on predictive (35) and master (36) model are given below.

$$Hue = 82.85 - 0.02M - 0.14T - 0.32RPM - 1.97(M * RPM) + 0.44(T * RPM) - 0.78RPM^2;\ R^2 = 0.7346 \quad \ldots (35)$$

$$Hue = 82.43 - 0.02M - 0.14T - 0.32RPM + 0.73M^2 + 0.55(M * T) - 1.97(M * RPM) - 0.57T^2 + 0.44(T * RPM) - 0.77RPM^2;\ R^2 = 0.9095 \quad \ldots (36)$$

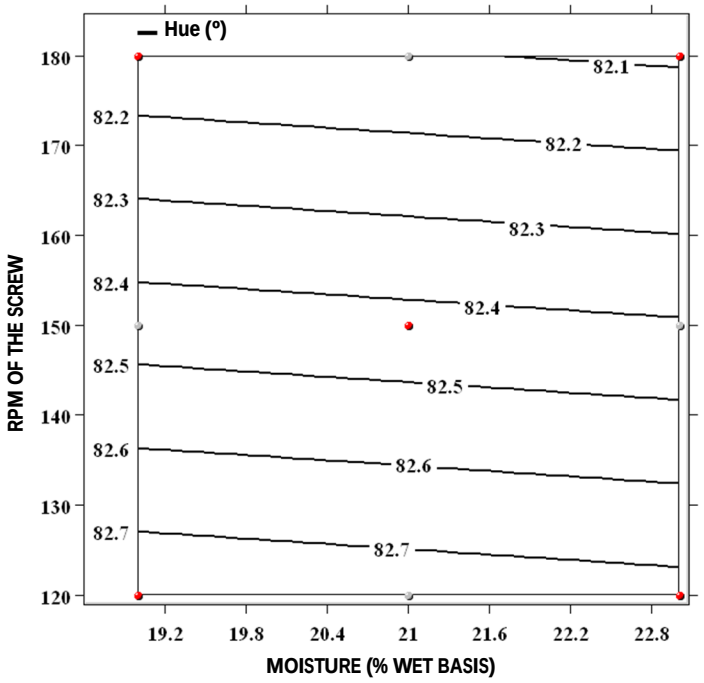

Figure 3.22 Contour plot for hue of extrudate at constant barrel temperature of 160 ºC.

Hue angle changed directly in proportion to the barrel temperature of the extruder. At lower temperature the extrudate has higher amount of redness, which can only be due to pigeonpea because Basmati rice does not impart red color to the product. At higher

temperature extrudate gets further cooked and product starts to turn brownish. Screw speed has a pronounced inverse effect on hue angle of the extrudate; this may be attributed to reduction in residence time at higher screw speed, reducing the browning of the extrudate.

3.16 Effect of extrusion conditions on chroma. (BBD)

In addition to being most influential factor for hue screw speed was found to be the most influential factor for chroma as well. The range of chroma was from 22.79 to 38.83. Figure 3.23 shows the effect of control variables on hue of the extrudate. The equations based on predictive (37) and master (38) model are given below

$$Chroma = 0.038 + 0.001RPM;\ R^2 = 0.2473 \quad \ldots (37)$$

$$Chroma = 0.038 + 0.002M - 0.002T + 0.001RPM + 0.003M^2 + 0.001(M * T) + 0.003(M * RPM) + 0.003(T * RPM);\ R^2 = 0.7843 \quad \ldots (38)$$

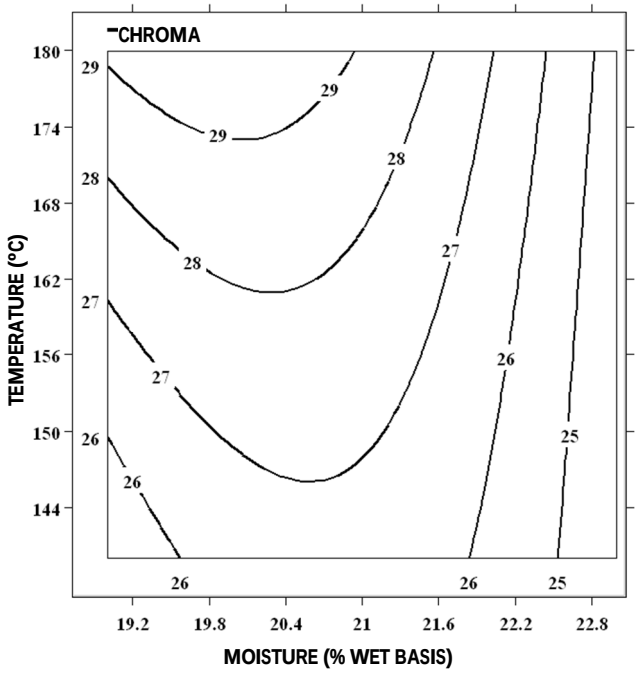

Figure 3.23 Contour plot for chroma of extrudate at constant screw speed of 150 RPM.

3.17 Residual analysis. (BBD)

As discussed earlier residual analysis was performed for this set of runs as well. Figure 3.23 to 3.27 shows the residual plot for sectional expansion index, breaking strength, breaking distance, hue and chroma respectively.

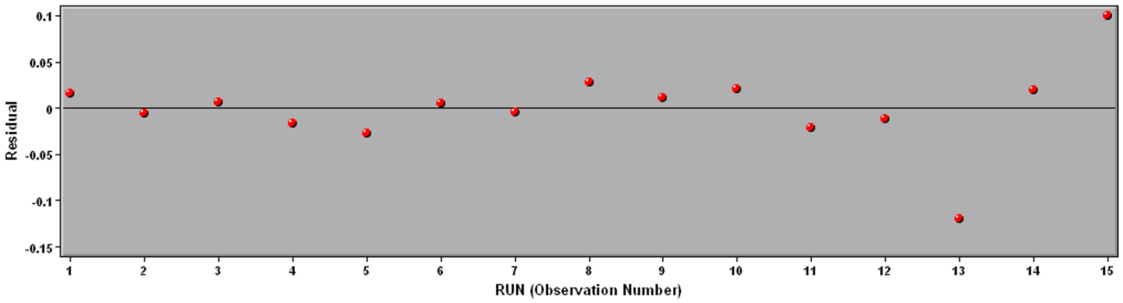

Figure 3.24 Residual plot for sectional expansion index of the extrudate. (BBD)

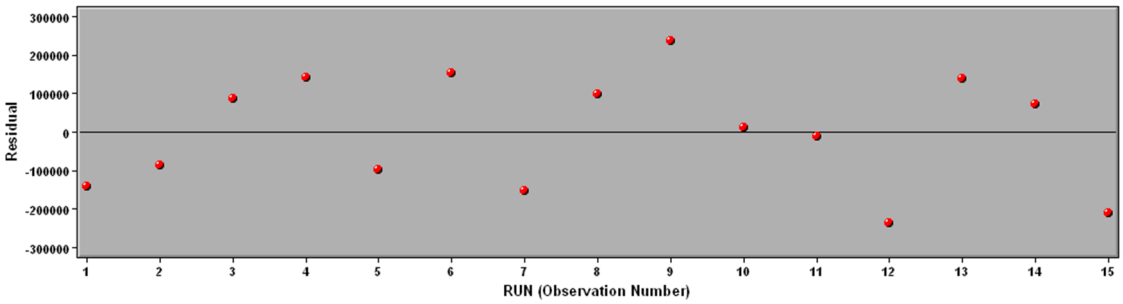

Figure 3.25 Residual plot for breaking strength of the extrudate. (BBD)

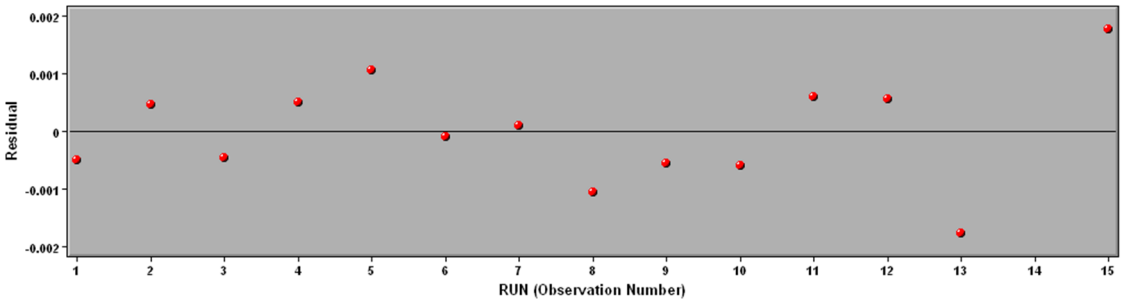

Figure 3.26 Residual plot for breaking distance of the extrudate. (BBD)

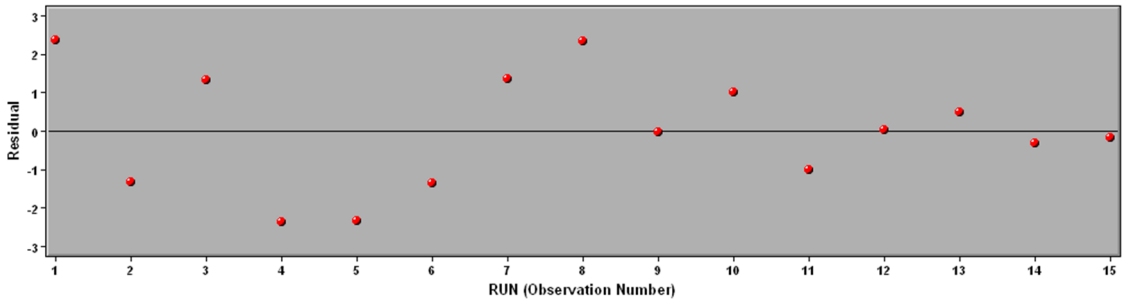

Figure 3.27 Residual plot for hue of the extrudate. (BBD)

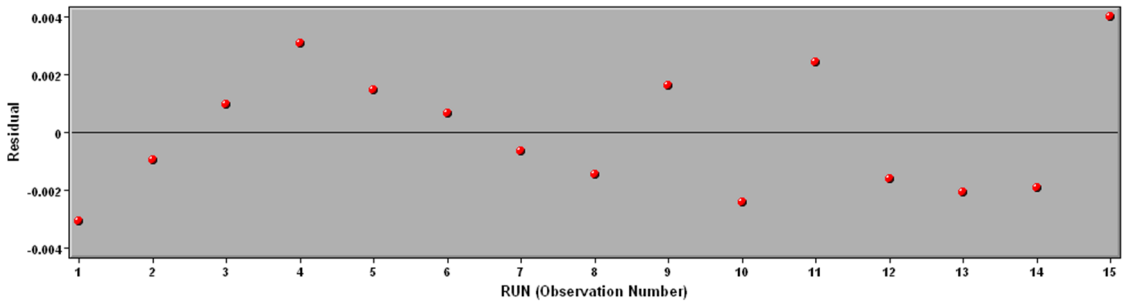

Figure 3.28 Residual plot for chroma of the extrudate. (BBD)

4. CONCLUSIONS

Preliminary trials with extrusion of pigeonpea validated that it was not possible to extrude pigeonpea by itself. Up to 23 % moisture on wet basis was added to the pigeonpea flour and still it was not possible to conduct the experiment. Beyond 23 % moisture on wet basis the texture of flour converted to dough making it difficult to mix and impossible to feed through extruder.

It was shown that pigeonpea can be extruded with the aid of Basmati rice. Operation range for amount of pigeonpea in the mix was found to be up to 75 % (wet basis) in terms of dry matter (i.e., excluding the moisture content of flour). Based on first set of runs of central composite design and validation from Box-Behnken design it was shown that ideal temperature range for the extrusion lies between 140 to 180 ºC.

In terms of protein content, higher amount of pigeonpea is beneficial, but in terms of extrusion operation and process reliability equal ratio of pigeonpea and Basmati rice was found to be ideal. This was validated in ease of operation during the experiments with set points of Box-Behnken design. Particle size distribution was found to be one of the major factors for most of the physico-chemical properties of extrudate. Moisture content of the finished product is directly proportional to moisture content of the initial product and is inversely proportional to the barrel temperature.

Increase in temperature and/or screw speed caused a decrease in bulk density of the extrudate.

Expansion of the product was directly related to barrel temperature and inversely related to the moisture content of the feed mixture.

Water solubility index (a measure of total dissolved solids) increased with increase in temperature. Amount of pigeonpea in the formulation had a direct correlation

with water solubility index. Breaking strength or stress resistance of extrudate increased with increase in amount of Basmati rice in the formulation. Increase in screw speed caused a decrease in breaking strength. Color of extrudate was found to be solely dependent on the screw speed. Increase in the screw speed resulted in decrease in the hue and chroma of the extrudate. This translates to extrudate being lighter in color and less brownish and more reddish in color.

One of the most important conclusions from this study was the effect of particle size distribution on finished product. It was shown that increasing particle size causes an increase in the expansion of extrudate. It also has an impact on bulk density and texture of the finished product. Ideal particle size distribution to achieve maximum expansion was found have a majority of the particles within 450 to 800 micrometer range.

To summarize our experiments, it is possible to extrude pigeonpea and a predictive model is available to identify operating condition optimized to deliver targeted physico-chemical properties. However, not a single set of condition can satisfy all physico-chemical criteria. Therefore it is necessary to approach the model with a flexible range for the desired physico-chemical property.

5. FUTURE WORK

Salt and pepper addition can influence the texture and sectional expansion index. Studies can be conducted to see these effects and identify optimum operating conditions and ratio of salt and pepper to be added.

Particle size distribution was found to have significant effect on water absorption index of extrudate. Studies can be conducted to evaluate the effect of particle size distribution on physico-chemical parameters of extrudate.

Cyclic testing could be applied to the texture analysis to evaluate chewiness characteristics of the extrudate.

Twin screw extrusion can provide better control over operating conditions and pre-conditioning of flour for moisture content can be avoided. Effect of twin screw extrusion on extrudate quality should be studied and optimum condition can be identified.

Possibility of extrusion of pigeonpea only can be studied on twin screw extruder.

Storage studies to evaluate change in texture and flavor of extrudate can be performed to see the stability and shelf life of extrudate.

A thorough market research on consumer preference and viability of the product needs to be conducted along with product optimization for salt, pepper and other spices.

Pigeonpea can be extruded with other cereal products to investigate the possibility of improvement in product characteristics.

6. REFERENCES

Achaya, K.T. 1998. Indian food: A historical companion. Oxford University Press, Delhi.

Agnesi, E. 1996. The history of pasta: Pasta and noodle technology. Ed. Kruger, J.E.; Matsuo, R.E.; Dick, J.W. AACC.

Akdogan, H.; Tomás, R.L. and Oliveira, J.C. 1997. Rheological properties of rice starch at high moisture contents during twin-screw extrusion. Lebenson Wiss Technol, 30:488-496

Anderson R.A.; Conway H.F. and Peplinski, A.J. 1970. Gelatinization of corn grits by roll cooking, extrusion cooking and steaming. Starch – Stärke, 22(4):130-135

Anonymous 1985. Introduction to powder characterization, An information booklet, p.2. Quantachrome Corp, Syosset, NY.

Atre, A. 2011. Masters thesis: Application of G*arcinia indica* as a colorant and antioxidant in rice extrudates. Food Science Department. Rutgers University

Azman. 1988. Quality of extrusion products made from rice-pigeonpea composite flour. (In Indonesian) M.S. thesis, Bogor Agricultural University, Bogor, Indonesia as mentioned in Damardjati, D. S. and Widowati, S. 1991. Utilization of pigeonpea and

other grain legumes in Indonesia. In ICRISAT: Uses of tropical grain legumes: proceedings of a consultants' meeting. pp:145-152.

Barron, C.; Bouchet, G.; Della Valle, D. J. and Planchot, V. 2001. Microscopical Study of the Destructuring of Waxy Maize and Smooth Pea Starches by Shear and Heat at Low Hydration. 33:289-300

Bean, M.M.; Nishita, K. D. 1985. Rice flours for baking. In Juliano BO, editor. Rice: chemistry and technology, 2nd ed. St. Paul:Amer Assoc of Cereal Chemists. P 539-556

Beetner, G.; Tsao, T.; Frey, A. and Lorenz, U. 1976. Stability of thiamine and riboflavin during extrusion processing of triticale. Journal of milk and food technology, 39:244-245

Berrios, J. J.; Wood, D. F.; Whitehand, L.; Pan, J. 2004. Sodium bicarbonate and the microstructure, expansion and color of extruded black beans. Journal of Food Processing and Preservation, 28:321-335

Blakeney, A. 1984 Rice grain quality. In: *Rice Growing in New South Wales* (edited by A. Currey). pp. 1-5 Yanco, Australia: Department of Agriculture New South Wales and Rice Research Committee

Box, G. E. P. and Behnken D. W. 1960, Some new three-level designs for the study of quantitative variables, Technometrics, 2:455-475

Box, G. E. P. and Wilson, K. B. 1951, On the experimental attainment of optimum conditions, Journal of the royal statistical society, Series B, 13:1-45

Campbell-platt, G. Editor: Food Extrusion Science and Technology. Wiley-Blackwell, West Sussex, United Kingdom, 2009

Chakraborty, S. K.; Singh, D. S.; Kumbhar, B. K. and Chakraborty, S. 2009. Process optimization with respect to the expansion ratios of millet and legume pigeonpea based extruded snacks. Journal of Food Process Engineering. 34:777-791

Chiang, B. Y.; Johnson, J. A. 1977. Measurement of total and gelatinized starch by glucoamylase and o-toluidine reagent. Cereal chemistry, 54(3):429-435

Chrastil, J. 1992. Correlation between the physicochemical and functional properties of rice. Journal of Agricultural and Food Chemistry 40(6):1683-1686

Degarmo, E. P.; Black, J T. and Kohser, R. A. 2003, Materials and Processes in Manufacturing (9th ed.), Wiley, p. 32, ISBN 0-471-65653-4

Drouzas, A. E. and Saravacos, G. D. 1988. Effective thermal conductivity of granular starch materials. Journal of food science, 53:1795-1799

Elias, L. G.; de Fernandez, D. G.; Bressani, R. 1979. Possible effects of seed coat polyphenols on the nutritional quality of bean protein. J Food Sci 44:524-527

Finch-Savage, W. E.; Leubner-Metzger, G. 2006. Tansley review: Seed dormancy and the control of germination. New Phytologist, 171:501-523

Frame, N. D. (editor)1994. The technology of extrusion cooking. Published by Blackie academic & professional, Glasgow, NZ

Geervani, P.; Theophilus, F. 1980. Effect of horne processing on nutrient composition of certain high yielding legume varieties. Ind J Nutr & Diet 17:443-446

Gorinstein, S.; Zemser, M.; Paredes, L. O. 1996. Structural stability of globulins. Journal of Agricultural Food Chemistry 44(1):100-105.

Harper, J. M. Extrusion of Foods, Volume 1 Boca Raton, FL: CRC Press, Inc. 1981

Hegde, K. T. M.; Karanth, R. V.; and Suchanthavong S.P. 1982. On the composition and technology of Harappan microbeads in Harappan Civilization. GL Possehl ed. Oxford and IBH publishing Co., New Delhi

Hodge, J. E.; Osman, E. M. In: Fenemma, O. (Editor), Principles of food science. Part 1: Food Chemistry. New York: Marcel Dekker, Inc., pp. 41-137 (1976)

Hulse, J. H. 1991. Nature, composition and utilization of grain legumes. In ICRISAT: uses of tropical grain legumes: proceedings of a consultants' meeting. pp:11-27

Iwe, M. O. 1998, Effects of extrusion cooking on functional properties of mixtures of full-fat soy and sweet potato, Plant foods for human nutrition, 53:37-46

Juliano, B. O. 1979. The chemical basis of rice grain quality. Proceedings of workshop on chemical aspects of rice grain quality. pp: 69-90. International Rice Research Institute, Los Baños, Laguna, Philippines

Juliano, B. O. 1982. Properties of rice starch in relation to varietal differences in processing characteristics of rice grain. Journal of Japan Society of Starch Science. 29:305-317

Juliano, B. O. (Editor). 1985. Rice Chemistry and Technology (2^{nd} edition). The American association of cereal chemists, Inc. St. paul, Minnesota, USA

Kokini, J. L.; Ho, C. T. and Karwe, M. V. (Editors) Food Extrusion Science and Technology, Marcel Dekker, Inc., New York, 1992.

Kumar, N.; Sarkar, B. C. and Sharma, H. K. 2010. Development and characterization of extruded product of carrot pomace rice flour and pulse powder. African Journal of Food Science. 4(11):703-717.

Ju, Z. Y.; Hettiarachchy, N. S.; Rath, N.2001. Extraction, Denaturation and Hydrophobic Properties of Rice Flour Proteins. 66(2):229-232

Karwe, M. V. “Food Extrusion,” chapter 5.10.4.9 under theme Food and Agricultural Engineering Resources, edited by G. V. Barbosa-Conovas and Pablo Juliano, in the Encyclopedia of Life Support Systems (EOLSS), developed under the auspices of the UNESCO, EOLSS Publishers, Oxford, UK, pp. 545-563, 2003.

KokiniKokini J.L., Cocero A.M., Madeka H., and de Graaf E. 1994. The development of state diagrams for cereal proteins. Trends in Food Science & Technology 5:281-288

Killeit, U. and Wiedmann, W. M. 1984. Einfluss der kochextrusion auf die stabilitat von B-vitaminen. Getreide, Brot und Mehl. 38:299-302

Kainuma, K. and French, D. 1971. Nägeli amylodextrin and its relationship to starch granule structure. I. Preparation and properties of amylodextrins from various starch types. Biopolymers. 10:1673-1680

Kite, F. E.; Schoch, T. J. and Leach, H. W. 1957 Granule swelling and paste viscosity of thick boiling starches. Baker's digest, 31(4):42-44

Liener, I. E. (1979) Protease inhibitors and leetins. In: Neuberger A, Jukes TH (eds). Biochemistry of nutrition. University Park Press, Baltimore, 27:97-122

Lowell, S.; Shields, J.; Thomas, M. and Thommes, M. 2006. Characterization of porous solids and powders: surface area, pore size and density 1st ed. (revised) Springer, Dordrecht, The Netherlands

Macke, S.J.R.J.; Gritt, D.T.; Consolmagno, S.J.G.J. 2010. Analysis of systematic error in ''bead method'' measurements of meteorite bulk volume and density. Planetary and space science, 58:421-426.

Marousis, S. N. and Saravacos, G. D. 1990. Density and porosity in drying starch materials. Journal of food science. 55:1367-1372

McGee, H. 1984. Cereal doughs and batters, in on food and cooking: the science and lore of the kitchen. Collier Books, Macmillan Publishing Co., New York

Mercier, C.; Linko, P.; Harper, J. M. 1989. Extrusion cooking. Published by A.A.C.C.,Inc. St. paul, Minnesota, USA

Merriam-Webster's Collegiate Dictionary (11th ed.), Springfield, MA, 2008

Morton, F. E. 1976. The pigeon pea (Cajanus cajan Millsp.): a high protein tropical bush legume. HortScience, 11 (1):11-19.

Nidhi, S. 2011. Master's thesis. Effect of processing on Pinhão seeds and extrudability of Pinhão flour. Food science department. Rutgers University.

Okpala, L. C. and Mamah, E. N. 2001. Functional properties of raw and processed pigeonpea (Cajanus cajan) flour. International Journal of Food Sciences and Nutrition. 52:343-346.

Price, M. L.; Hagerman, A. E. and Butler, L. G. 1980. Tannin content of cowpeas, chickpeas,
pigeonpea and mung beans. J Agri Food Chern 28:459-461

Rampersad, R.; Badrie, N. and Comissiong, E. 2003 Physico-chemical and sensory characteristics of flavored snacks from extruded cassava/pigeonpea flour. Journal of food science, 68: 363-367

Rao, S. K. 1989. Effect of extrusion on lipid oxidation. Journal of Food Science. 54(6):1580-1583

Ratnayake, W. S.; Jackson, D. S. 2007. A new insight into the gelatinization process of native starches. 67:511-529

Sekhar, B.P.S. and Reddy, G. M. 1982. Amino acid profiles in some scented rice varieties. Theoretical and Applied Genetics

Theoretical and Applied Genetics, 62:35-37

Reddy LJ, Green JM, Singh D, Eisen SS, Jambunathan R. 1979 Seed protein studies on Cajanus cajan Atylosia spp. and some hybrid derivatives. In: Proc Sym Seed protein improvement in cereals and grain legumes. lAEA/FAO, Munich, West Germany pp 105-117

Riaz, M. N. 2000. Extruders in food applications. 1st edition, Lancaster, PA, Technomic Publishing Company, Inc.

Shah, K. K. 1996. Ph.D. thesis titled Thermal conductivity of porous, hygroscopic food powders under extrusion conditions. Rutgers, the state university of New Jersey

Singh U (1984) The inhibition of digestive enzymes by polyphenols of chickpea (Cicer arietinum L.) and pigeonpea (Cajanus cajan L.). Nut Rep Int 29:745-753

Singh, N.; Kaur, L.; Sandhu, K.S.; Kaur, J.; Nishinari, K. 2005. Relationships between physicochemical, morphological, thermal, rheological properties of rice starches. Food hydrocolloids. 20:532-542

Singh, U.; Eggum, B. O. 1984. Factors affecting the protein quality of pigeonpea (Cajanus cajan L.) 34:273-283

Singh, U. ;Jambunathan, R. 1980. A survey of the methods of milling and consumer acceptance of pigeonpeas in India. In Proc International Workshop on pigeonpeas. Vol 2, p 149, 15-19 Dec, 1980. ICRISAT Center, Patancheru, A.P. 502 324, India

Singh, U.; Jambunathan, R. 1982 Distribution of seed protein fractions and amino acids in different anatomical parts of chickpea (Cicer arietinum L.) and pigeonpea (Cajanus cajan L.). Qual Plant Plant Foods Hum Nutr 31 :347-354

Van den einde, R.; Van Der Linedn, E.; Van Der Goot, A. J.; Boom, R. 2004. A mechanistic model of the relation between molecular structure of amylopectin and macromolecular degradation during heating-shearing process. 85:589-594

Van der Maesen, L. J. G. 1980. India is the native home of the pigeonpea. Pages 257-262 in Arends JC, G Boelema, CT de Groot, and AJM Leeuwenberg (eds). Liber gratulations in honoram HCD de wit. Miscellaneous papers 19. Wageningen, Netherlands.

Whiteman, P. C.; Byth, D. E. and Wallis, E. S. 1985. pigeonpea. In grain legume crops. Summerfield, R. J.; Roberts, E. H. (editor) pp. 698–698. Collins Professional and Technical Books. London.

Woodcock, C.R.; Mason, J.S. 1987. Bulk solids handling, an introduction to the practice and technology, Blackie & Son Ltd.

X-RITE. 1993. A guide to understanding color communication. X-Rite Form L10-001 (Rev.8-90). P/N918-801. X-Rite Inc., Grandville, MI

Ziggers, D. 2000. Good preconditioning with half of the extruding. Feed tech., 4(10):20-21.

Zobel, H. F. 1964. X-ray analysis of starch granules. in: Methods in carbohydrate chemistry. 4:109-113. R. L. Whistler (editor) Academic press, Inc. New York.

APPENDIX

Example of a datasheet generated by SAS v9.2 for statistical analysis

ADX Report for 1 Final

Today's date: 19AUG2011
Experiment creation date: 19AUG2011

DESIGN DETAILS

Design type: Response Surface
Design description: Central Composite: Orthogonal
Number of factors: 4
Number of runs: 30
Number of blocks: 3

FACTORS

Factors and Levels:

Factor	Low	Center	High
RATIO	0.25	0.5	0.75
MOISTURE	19	21.5	24
RPM	120	150	180
TEMPERAT	120	140	160

RESPONSE

Response
AMP
PSI
GPERMIN
DMOIST
D1MOIST
SEI
BD
PD
WSI
WAI
TEXTURE

BLOCK INFORMATION

Block name: BLOCK
Number of blocks: 3
Block levels: 1
2
3

DESIGN POINTS (Coded)

RUN	BLOCK	RATIO	MOISTURE	RPM	TEMPERAT	AMP	PSI	GPERMIN	DMOIST	D1MOIST	SEI	BD	PD	WSI	WAI	TEXTURE
1	1	-1	-1	1	8.0	2980.0	187.00	10.87	6.52	1.53	1.40	1.65	9.21	3.01	3.80					
2	1	-1	-1	-1	8.0	3560.0	200.00	10.20	3.18	1.21	1.28	1.57	9.41	3.14	4.69					
3	1	-1	1	-1	6.2	1840.0	125.46	14.21	7.13	1.17	1.35	1.67	6.22	3.24	5.64					
4	1	-1	1	1	4.0	1140.0	101.54	8.95	5.59	1.61	0.78	1.50	11.38	4.28	3.17					
5	1	1	-1	-1	4.0	1125.0	12.57	5.25	5.05	1.35	1.29	1.57	16.94	3.53	12.10					
6	1	1	-1	1	1.0	270.0	100.40	12.51	7.82	1.86	0.81	1.51	24.20	3.83	6.94					
7	1	1	1	-1	2.0	500.0	10.51	13.38	6.77	1.20	1.26	1.62	10.63	3.73	10.90					
8	1	1	1	1	2.0	330.0	5.83	12.58	6.10	1.63	0.89	1.51	13.92	3.82	3.74					
9	1	0	0	0	7.0	1730.0	158.82	10.84	5.28	1.33	1.09	1.59	14.30	3.45	4.01					
10	1	0	0	0	7.0	1768.0	131.20	13.27	5.77	1.35	0.99	1.57	13.59	3.75	3.20					
11	2	-1	-1	-1	8.2	2000.0	138.00	8.54	4.95	1.43	1.16	1.54	7.27	3.75	8.06					
12	2	-1	-1	1	6.4	2710.0	188.02	11.19	5.33	1.82	0.70	1.62	13.06	4.24	1.75					
13	2	-1	1	-1	2.2	755.0	41.35	14.99	7.03	1.97	0.69	1.51	11.61	4.99	2.54					
14	2	-1	1	1	5.0	1776.0	107.69	12.42	5.26	1.57	0.85	1.62	4.40	4.33	4.63					
15	2	1	-1	-1	4.0	838.5	26.33	10.21	6.06	2.42	0.42	1.53	27.80	4.31	1.26					
16	2	1	-1	1	6.0	1820.0	64.63	11.61	4.41	1.52	0.60	1.52	15.47	4.12	2.28					
17	2	1	1	-1	4.0	1530.0	53.07	12.35	4.47	1.34	1.05	1.57	15.99	3.43	3.12					
18	2	1	1	1	4.0	490.0	53.28	12.46	3.56	2.00	0.57	1.52	27.69	4.35	1.08					
19	2	0	0	0	9.0	2840.0	132.00	14.71	8.39	1.89	0.75	1.58	16.41	3.85	2.50					
20	2	0	0	0	6.0	1960.0	181.50	13.98	7.90	1.50	0.90	1.54	13.75	3.47	5.20					
21	3	-1	0	0	5.0	1500.0	109.50	12.68	3.69	1.70	0.85	1.56	9.39	4.81	3.36					
22	3	1	0	0	2.5	1258.0	33.60	12.90	7.00	2.04	0.75	1.50	23.57	4.30	0.02					
23	3	0	-1	0	6.0	600.0	118.00	10.54	3.79	2.13	0.63	1.57	16.09	4.12	1.60					
24	3	0	1	0	7.0	1650.0	236.00	11.88	3.13	1.71	0.83	1.67	9.61	4.36	2.55					
25	3	0	0	-1	6.0	1800.0	108.10	11.65	4.73	1.52	0.89	1.57	13.01	4.28	3.63					
26	3	0	0	1	4.0	1500.0	160.00	13.28	2.37	1.34	1.25	1.48	12.96	3.31	3.38					
27	3	0	0	0	10.0	2540.0	182.00	10.48	4.83	1.24	0.98	1.60	12.20	3.42	4.12					
28	3	0	0	0	5.5	1500.0	261.00	10.41	3.81	1.77	0.86	1.52	18.46	4.38	2.10					
29	3	0	0	0	6.0	1500.0	156.00	10.44	5.31	1.82	0.73	1.66	13.79	4.48	2.26					
30	3	0	0	0	6.0	1300.0	154.00	10.24	3.26	1.67	0.69	1.64	13.80	4.23	2.58					

DESIGN POINTS (Uncoded)

RUN	BLOCK	RATIO	MOISTURE	RPM	TEMPERAT	AMP	PSI	GPERMIN	DMOIST	D1MOIST	SEI	BD	PD	WSI	WAI	TEXTURE
1	1	0.25	19.0	120	160	8.0	2980.0	187.00	10.87	6.52	1.53	1.40	1.65	9.21	3.01	3.80					
2	1	0.25	19.0	180	120	8.0	3560.0	200.00	10.20	3.18	1.21	1.28	1.57	9.41	3.14	4.69					
3	1	0.25	24.0	120	120	6.2	1840.0	125.46	14.21	7.13	1.17	1.35	1.67	6.22	3.24	5.64					
4	1	0.25	24.0	180	160	4.0	1140.0	101.54	8.95	5.59	1.61	0.78	1.50	11.38	4.28	3.17					
5	1	0.75	19.0	120	120	4.0	1125.0	12.57	5.25	5.05	1.35	1.29	1.57	16.94	3.53	12.10					
6	1	0.75	19.0	180	160	1.0	270.0	100.40	12.51	7.82	1.86	0.81	1.51	24.20	3.83	6.94					
7	1	0.75	24.0	120	160	2.0	500.0	10.51	13.38	6.77	1.20	1.26	1.62	10.63	3.73	10.90					
8	1	0.75	24.0	180	120	2.0	330.0	5.83	12.58	6.10	1.63	0.89	1.51	13.92	3.82	3.74					
9	1	0.50	21.5	150	140	7.0	1730.0	158.82	10.84	5.28	1.33	1.09	1.59	14.30	3.45	4.01					
10	1	0.50	21.5	150	140	7.0	1768.0	131.20	13.27	5.77	1.35	0.99	1.57	13.59	3.75	3.20					
11	2	0.25	19.0	120	120	8.2	2000.0	138.00	8.54	4.95	1.43	1.16	1.54	7.27	3.75	8.06					
12	2	0.25	19.0	180	160	6.4	2710.0	188.02	11.19	5.33	1.82	0.70	1.62	13.06	4.24	1.75					
13	2	0.25	24.0	120	160	2.2	755.0	41.35	14.99	7.03	1.97	0.69	1.51	11.61	4.99	2.54					
14	2	0.25	24.0	180	120	5.0	1776.0	107.69	12.42	5.26	1.57	0.85	1.62	4.40	4.33	4.63					
15	2	0.75	19.0	120	160	4.0	838.5	26.33	10.21	6.06	2.42	0.42	1.53	27.80	4.31	1.26					
16	2	0.75	19.0	180	120	6.0	1820.0	64.63	11.61	4.41	1.52	0.60	1.52	15.47	4.12	2.28					
17	2	0.75	24.0	120	120	4.0	1530.0	53.07	12.35	4.47	1.34	1.05	1.57	15.99	3.43	3.12					
18	2	0.75	24.0	180	160	4.0	490.0	53.28	12.46	3.56	2.00	0.57	1.52	27.69	4.35	1.08					
19	2	0.50	21.5	150	140	9.0	2840.0	132.00	14.71	8.39	1.89	0.75	1.58	16.41	3.85	2.50					
20	2	0.50	21.5	150	140	6.0	1960.0	181.50	13.98	7.90	1.50	0.90	1.54	13.75	3.47	5.20					
21	3	0.25	21.5	150	140	5.0	1500.0	109.50	12.68	3.69	1.70	0.85	1.56	9.39	4.81	3.36					
22	3	0.75	21.5	150	140	2.5	1258.0	33.60	12.90	7.00	2.04	0.75	1.50	23.57	4.30	0.02					
23	3	0.50	19.0	150	140	6.0	600.0	118.00	10.54	3.79	2.13	0.63	1.57	16.09	4.12	1.60					
24	3	0.50	24.0	150	140	7.0	1650.0	236.00	11.88	3.13	1.71	0.83	1.67	9.61	4.36	2.55					
25	3	0.50	21.5	120	140	6.0	1800.0	108.10	11.65	4.73	1.52	0.89	1.57	13.01	4.28	3.63					
26	3	0.50	21.5	180	140	4.0	1500.0	160.00	13.28	2.37	1.34	1.25	1.48	12.96	3.31	3.38					
27	3	0.50	21.5	150	120	10.0	2540.0	182.00	10.48	4.83	1.24	0.98	1.60	12.20	3.42	4.12					
28	3	0.50	21.5	150	160	5.5	1500.0	261.00	10.41	3.81	1.77	0.86	1.52	18.46	4.38	2.10					
29	3	0.50	21.5	150	140	6.0	1500.0	156.00	10.44	5.31	1.82	0.73	1.66	13.79	4.48	2.26					
30	3	0.50	21.5	150	140	6.0	1300.0	154.00	10.24	3.26	1.67	0.69	1.64	13.80	4.23	2.58					

FIT DETAILS FOR WSI:

WSI Check Assumptions Analysis

Response Transformation
Optimal power from Box-Cox plot: WSI**0.6
Power recommended by ADX: WSI
Power applied for response transformation: WSI
Response Scaling Shift: 0

Outlier Observations
Outlier statistic: Poutlier
Outlier criterion: 0.05
Run numbers deleted from analysis: 2,7

Influential Observations
Influential statistic: Dffits
Influential criterion: 2
Run numbers deleted from analysis: None

ANOVA for WSI

	Master Model				Predictive Model				
Source	DF	SS	MS	F	Pr > F	DF	SS	MS	F	Pr > F
BLOCK	2	1.640937	0.820468	0.286493	0.7563	2	12.4566	6.2283	1.603925	0.2228
RATIO	1	591.1365	591.1365	206.4145	<.0001	1	627.5138	627.5138	161.5987	<.0001
MOISTURE	1	3.971511	3.971511	1.386782	0.2638					
RPM	1	1.124314	1.124314	0.392591	0.5437					
TEMPERAT	1	233.1036	233.1036	81.3957	<.0001	1	249.0487	249.0487	64.13555	<.0001
RATIO*RATIO	1	11.57271	11.57271	4.040987	0.0696					
RATIO*MOISTURE	1	0.064838	0.064838	0.02264	0.8831					
RATIO*RPM	1	0.572818	0.572818	0.200018	0.6634					
RATIO*TEMPERAT	1	5.819167	5.819167	2.031951	0.1818					
MOISTURE*MOISTURE	1	5.085378	5.085378	1.775725	0.2096					
MOISTURE*RPM	1	0.017608	0.017608	0.006148	0.9389					
MOISTURE*TEMPERAT	1	0.846618	0.846618	0.295624	0.5975					
RPM*RPM	1	4.180782	4.180782	1.459856	0.2523					
RPM*TEMPERAT	1	0.522626	0.522626	0.182492	0.6775					
TEMPERAT*TEMPERAT	1	2.591207	2.591207	0.904804	0.3619					
Model	16	860.3435	53.77147	18.77606	<.0001	4	802.5329	200.6332	51.66749	<.0001
Error	11	31.50215	2.863832			23	89.31272	3.883162		
(Lack of fit)	8	27.71225	3.464031	2.74205	0.2195	10	51.25587	5.125587	1.750871	0.1704
(Pure Error)	3	3.7899	1.2633			13	38.05685	2.92745		
Total	27	891.8456				27	891.8456			

Fit Statistics for WSI

	Master Model	Predictive Model
Mean	14.50321	14.50321
R-square	96.47 %	89.99 %
Adj. R-square	91.33 %	88.24 %
RMSE	1.692286	1.970574
CV	11.66835	13.58715

Alias Structure for WSI

Master Model	Predictive Model
(BLOCK='1') - (BLOCK='3')	(BLOCK='1') - (BLOCK='3')
(BLOCK='2') - (BLOCK='3')	(BLOCK='2') - (BLOCK='3')

Predictive Model for WSI

Coded Levels(-1,1):

WSI = 14.288 - 0.568*(BLOCK='1') + 1.057*(BLOCK='2') + 6.312063*RATIO
+ 3.976508*TEMPERAT

Uncoded Levels:

WSI = -26.1717 - 0.568*(BLOCK='1') + 1.057*(BLOCK='2') + 25.24825*RATIO
+ 0.198825*TEMPERAT

Effect Estimates for WSI

	Master Model				Predictive Model			
Term	Estimate	Std Err	t	Pr > |t|	Estimate	Std Err	t	Pr > |t|
(BLOCK='1')	-0.251647	1.336295	-0.18832	0.8541	-0.568	0.934725	-0.60767	0.5494
(BLOCK='2')	0.7829412	1.085921	0.720993	0.4860	1.057	0.881267	1.199409	0.2426
RATIO	6.2776667	0.436946	14.36713	<.0001	6.3120635	0.496538	12.71215	<.0001
MOISTURE	-0.514556	0.436946	-1.17762	0.2638				
RPM	-0.273778	0.436946	-0.62657	0.5437				
TEMPERAT	3.9421111	0.436946	9.021957	<.0001	3.9765079	0.496538	8.008467	<.0001
RATIO*RATIO	2.1829412	1.085921	2.010221	0.0696				
RATIO*MOISTURE	0.1540074	1.023531	0.150467	0.8831				
RATIO*RPM	-0.457757	1.023531	-0.44723	0.6634				
RATIO*TEMPERAT	1.4590074	1.023531	1.425465	0.1818				
MOISTURE*MOISTURE	-1.447059	1.085921	-1.33256	0.2096				
MOISTURE*RPM	-0.080257	1.023531	-0.07841	0.9389				
MOISTURE*TEMPERAT	0.5565074	1.023531	0.543713	0.5975				
RPM*RPM	-1.312059	1.085921	-1.20824	0.2523				
RPM*TEMPERAT	0.4372426	1.023531	0.427191	0.6775				
TEMPERAT*TEMPERAT	1.0329412	1.085921	0.951212	0.3619				

Picture of extrudates produced during Box-Behnken design runs

21% Moisture (wet basis) 160°C 150RPM | 21% Moisture (wet basis) 160°C 150RPM | 23% Moisture (wet basis) 160°C 120RPM | 21% Moisture (wet basis) 160°C 150RPM | 23% Moisture (wet basis) 180°C 150RPM

23% Moisture (wet basis) 140°C 150RPM | 19% Moisture (wet basis) 160°C 180RPM | 23% Moisture (wet basis) 160°C 180RPM | 19% Moisture (wet basis) 140°C 150RPM | 19% Moisture (wet basis) 180°C 150RPM

21% Moisture (wet basis) 140°C 180RPM | 21% Moisture (wet basis) 180°C 180RPM | 19% Moisture (wet basis) 160°C 120RPM | 21% Moisture (wet basis) 140°C 120RPM | 21% Moisture (wet basis) 180°C 120RPM

Typical Force vs. distance diagram for breaking strength analysis

Brookfield Texture Analyzer CT3 Volodkevitch bite jaw, speed: 1 mm/s